Toward a quantitative understanding of mechanical behavior of nanocrystalline metals

Dao, M.; Lu, L.; Asaro, R. J.; De Hosson, J.T.M.; Ma, E.

Published in:
Acta Materialia

DOI:
10.1016/j.actamat.2007.01.038

Publication date:
2007

Available online at www.sciencedirect.com
ScienceDirect
Acta Materialia 55 (2007) 4041–4065
Acta MATERIALIA
www.elsevier.com/locate/actamat

Overview No. 143

Toward a quantitative understanding of mechanical behavior of nanocrystalline metals

M. Dao [a,*], L. Lu [b], R.J. Asaro [c], J.T.M. De Hosson [d], E. Ma [e]

[a] Department of Materials Science and Engineering, Massachusetts Institute of Technology, Cambridge, MA 02139, USA
[b] Shenyang National Laboratory for Materials Science, Institute of Metal Research, Chinese Academy of Sciences, Shenyang 110016, China
[c] Department of Structural Engineering, University of California, San Diego, CA 92093, USA
[d] Department of Applied Physics, Netherlands Institute for Metals Research and Materials Science Center, University of Groningen, 9747 AG, Groningen, The Netherlands
[e] Department of Materials Science and Engineering, John Hopkins University, Baltimore, MD 21218, USA

Received 19 August 2006; received in revised form 23 January 2007; accepted 24 January 2007
Available online 28 March 2007

Abstract

Focusing on nanocrystalline (nc) pure face-centered cubic metals, where systematic experimental data are available, this paper presents a brief overview of the recent progress made in improving mechanical properties of nc materials, and in quantitatively and mechanistically understanding the underlying mechanisms. The mechanical properties reviewed include strength, ductility, strain rate and temperature dependence, fatigue and tribological properties. The highlighted examples include recent experimental studies in obtaining both high strength and considerable ductility, the compromise between enhanced fatigue limit and reduced crack growth resistance, the stress-assisted dynamic grain growth during deformation, and the relation between rate sensitivity and possible deformation mechanisms. The recent advances in obtaining quantitative and mechanics-based models, developed in line with the related transmission electron microscopy and relevant molecular dynamics observations, are discussed with particular attention to mechanistic models of partial/perfect-dislocation or deformation-twin-mediated deformation processes interacting with grain boundaries, constitutive modeling and simulations of grain size distribution and dynamic grain growth, and physically motivated crystal plasticity modeling of pure Cu with nanoscale growth twins. Sustained research efforts have established a group of nanocrystalline and nanostructured metals that exhibit a combination of high strength and considerable ductility in tension. Accompanying the gradually deepening understanding of the deformation mechanisms and their relative importance, quantitative and mechanisms-based constitutive models that can realistically capture experimentally measured and grain-size-dependent stress–strain behavior, strain-rate sensitivity and even ductility limit are becoming available. Some outstanding issues and future opportunities are listed and discussed.

Keywords: Nanocrystalline materials; Mechanical properties; Plastic deformation; Grain boundaries; Modeling

1. Introduction

In the mid-1980s, Gleiter [1] made the visionary argument that metals and alloys, if made nanocrystalline, would have a number of appealing mechanical characteristics of potential significance for structural applications. This followed, quite plausibly, from what was known about the extraordinary strength of alloys such as highly cold drawn wires characterized by structural length scales of nanometer size (e.g. [2]). Compared with conventional coarser grained materials, the benefits that may be derived from nanostructuring include ultrahigh yield and fracture strengths, superior wear resistance, and possibly superplastic formability at low temperatures and/or high strain rates. The deformation mechanisms are also predicted to be radically different, as plasticity at the nanoscale may be mediated mostly by grain-boundary deformation

* Corresponding author. Tel.: +1 617 253 2100; fax: +1 617 258 0390.
E-mail address: mingdao@mit.edu (M. Dao).

1359-6454/$30.00
doi:10.1016/j.actamat.2007.01.038

processes. These provocative thoughts stimulated widespread interest in the mechanical properties and novel deformation mechanisms of nanostructured materials over the past two decades. Many research articles have been published in this area. Unfortunately, most of the experimental findings documented in this literature up to the late 1990s were not representative of intrinsic material response, due to the problems and difficulties associated with preparing full-density and flaw-free nanocrystalline samples [3]. Improvements in materials processing, discussed briefly herein, have led to enhancements in properties, but yet still further refinements are needed.

Strengthening with grain size refinement in metals and alloys with an average grain size of 100 nm or larger has been well characterized by the Hall–Petch (H–P) relationship, where dislocation pile-up against grain boundaries (GBs) along with other transgranular dislocation mechanisms are the dominant strength-controlling processes. When the average, and entire range of, grain sizes is reduced to less than 100 nm, the dislocation operation becomes increasingly more difficult and grain boundary-mediated processes become increasingly more important [3–6].

With these observations in mind, we continue to use the terminology proposed in the earlier literature [3]: nanocrystalline (nc) materials are defined as those with their average and entire range of grain size typically finer than 100 nm; ultrafine crystalline (ufc) materials are defined as those with grain sizes on the order of 100 nm–1 μm; and microcrystalline (mc) materials are defined as those with average grain sizes greater than 1 μm [3–5,7–9]. When one or more dimensions on average is smaller than 100 nm, the material is often termed a nanostructured (ns) material [7,8,10]. Another category may be termed nc/ufc metals, whose grain sizes are characterized by averages near 100 nm, but with grain size distributions spanning the range from nc to 500 nm. This class is included to highlight the fact that recent methods utilizing severe plastic deformation methods have produced high-density bulk Ti metal with grain sizes (d) in the range of $50\ \text{nm} \leqslant d \leqslant 150\ \text{nm}$.

A number of reviews have been written since Gleiter [1] first summarized the pioneering ideas, e.g. by Gleiter [11,12], Weertman [13], Kumar et al. [3], Koch [4], Cheng et al. [14], Wolf et al. [15], Meyers et al. [9], Ma [10], etc. Specific references to these are made throughout the text.

This overview highlights some of the most recent experimental advances in property improvements and mechanisms-based quantitative analyses, rather than attempting to provide a detailed account for all developments in this field. Recent experimental studies, discussed herein, on the one hand point out promising routes to optimize mechanical properties, yet on the other hand reveal challenges to the understanding of intrinsic nc behavior that require further careful quantitative examination. Examples of such effects or phenomena include grain size distribution vs. overall mechanical response and properties, the unusual size dependence of nanoscale growth twins in terms of ductility and the (apparent) stress-induced grain growth observed during deformation. All of these have significant effects on the macroscopic mechanical response and (therefore) implications for potential use of nc or even ufc metals and alloys. Parallel to these new developments in experimental investigations, several recent mechanisms based and physically motivated models have provided quantitative insights into the deformation mechanisms as well as possible routes to mechanical property improvements.

This paper is organized as follows. Section 2 briefly highlights several of the most important and commonly used methods for processing bulk nc/ns materials. Severe plastic deformation is included in the discussion owing to the aforementioned ability to process nc/ufc metals. Although not intended as a comprehensive review of processing, this discussion provides needed perspective for our subsequent presentation of nc metal properties. Section 3 summarizes experimental observations on strength, ductility, strain rate and temperature dependence of strength, fatigue and tribological properties of nc materials. Here, along with the discussion of recently reported phenomenology, we note several key findings that challenge our understanding of nc metal behavior. Nanocrystalline grain size stability during deformation is one example of such critical behavior. Improvements in fatigue performance, including crack initiation vs. fatigue crack growth, are additional examples. Section 4 reviews recent developments in dislocation based and physically motivated continuum models. The modeling is discussed with an aim to quantitatively explore the critical phenomenology highlighted in Section 3. This focus explains the choice of our title. A summary and concluding remarks follow in Section 5.

2. Materials processing

In evaluating and optimizing the performance of an nc or ns metal, it is essential to control the defect content as well as the microstructure or perhaps more precisely the "nanostructure". In particular, grain size distribution, the distribution of interface misorientation angles, residual stresses and internal strains are among the important structural features. In the past, the low Young's modulus of nanostructured materials has been attributed to the unusual grain-boundary structures present but this phenomenon is also influenced by defect structure, such as porosity [16]. Further, it can be anticipated that control of the grain-size distribution is extremely important in the experimental design of nc materials. Grain size distribution is, in fact, considered both experimentally and theoretically later in this review.

Nanocrystalline materials can be processed through either a bottom-up approach [1,17,18], where the nanostructure is built atom by atom and layer by layer, or a top-down approach, where the nanostructure is synthesized by breaking down the bulk microstructure into the nanoscale [7,19]. Several major processing techniques have been successfully applied so far: (1) inert gas condensation

(IGC) [1,17,18], (2) mechanical milling/alloying [19–21], (3) electrodeposition (ED) [22–25], (4) crystallization from amorphous materials [26] and (5) severe plastic deformation (SPD) of bulk metals [7,8]. It has also been proven that the grain-size distribution of nc metals can be controlled by a so-called nanocluster source using gas aggregation and condensation [27–31]. In addition, surface engineering methods have been explored such as physical vapor deposition, chemical vapor deposition and high-power laser treatments to synthesize, in particular, nanocomposite (metallic) materials [32].

The oldest preparation methods of nanostructured metals and alloys are IGC [33,34] and ball milling [35], but soon after their introduction several drawbacks were noted. Material prepared with IGC showed a large porosity and the manufacturing output was rather small despite relatively high costs of the preparation equipment. Likewise, ball milling, well known from the production of amorphous metals, tends to produce nanostructured materials with considerable lattice distortions and high impurity contents. Both gas condensation and mechanical milling are capable of producing material with grain sizes below 100 nm; nevertheless, the principal disadvantage is that residual porosity may still remain as a compaction step is needed to reach the bulk form. These thermally assisted compaction processes that follow gas condensation and milling methods lead to unwanted grain growth. For industrial applications more cost-effective preparation techniques are required and none of these earlier approaches actually survived easily in the field of application. Of the aforementioned panoply of methods, three methods have emerged with greater potential: electrodeposition, severe plastic deformation and cluster deposition techniques.

The method of electrodeposition has several advantages and, interestingly, is quite an old technique. Electrodeposits with special properties were already being prepared in the middle of the 19th century [36] and, at the turn of the 20th century, electrolysis was employed to produce special coatings with an enhanced hardness [37]. Electrochemical deposition of nanostructured metals is possible, provided a considerable number of grain nuclei are created on the electrode surface. Further, the growth of nuclei and crystallites should be strongly suppressed. The former requirement is addressed by the use of high current densities ($2\ A/cm^{-2}$) that are not possible in direct current (DC) plating. Although the peak current density is fairly high in the so-called pulsed electrolysis, the duration of the pulse lies in the millisecond range and requires a low voltage, i.e. comparable to the voltage used in DC plating [38]. As a consequence, grain size reduction can be achieved with a short duration of the pulse combined with high peak current densities. Second, grain size reduction is promoted by the use of an electrolyte that contains additives. The additive molecules which adsorb on active sites of the electrode accelerate the grain nucleation and reduce the crystallite growth. Third, the grain size can be controlled by the bath temperature, since at lower temperatures a slower surface diffusion of adatoms causes retarded grain growth. Along these lines, nanocrystalline Ni was electrochemically prepared by Erb and co-workers [23,39] and by Bakonyi et al. [40,41] using electrolysis. DC electrolysis provides materials with some growth texture and with grain sizes of 30 nm and above. In contrast, pulsed procedures produce texture-free and pore-free nanostructured metals with grain diameters clearly below 20 nm. Besides pure metals like Ni, Pd and pure Cu with nanoscale growth twins [25], nanocrystalline NiCu alloys were also manufactured using a pulse electroplating technique [38]. Another new development worth mentioning is that, by precisely controlling the W content and thereby controlling the grain size (~2–140 nm) in making electrodeposited nc Ni–W alloys [42], plastically graded nc Ni–W samples can be successfully produced [43,44].

As regards the other two promising techniques, severe plastic deformation (SPD) produces a relatively large amount of bulk material that can be 100% dense [7]. This is a major advantage, especially for mechanical property measurements and structural applications [7,8]. Many ns metals and alloys have been processed, and intensive studies of such ns/ufc metals are ongoing worldwide. But for pure face-centered cubic (fcc) metals the smallest grain size achievable via SPD is often above the 100 nm limit, so the interesting mechanical properties of these SPD nc/ufc materials will not be discussed at length in this overview. After SPD, the grain size distribution can be somewhat broad, ranging between tens and a few hundred nanometers up to 1000 nm in the most extreme cases, when processing is not optimized; also, some grain boundaries are not of the high-angle type. Surface mechanical attrition treatment (SMAT) is another recently developed SPD-related technique that can induce grain refinement into a nanometer regime in the surface layer of bulk materials [45,46]. As a simple and flexible approach for obtaining nanostructures, SMAT is potentially useful in industrial applications, and it provides a unique opportunity to investigate the severe plastic deformation-induced grain refinement process [47,48]. In comparison, both the electrodeposition method and (nano)cluster source method generate fully dense nc metals with grain sizes down to a few nanometers, and have a relatively narrow grain size distribution [28,49]. Interestingly, the clusters produced by the cluster-source method are grown in extreme non-equilibrium conditions, which allow metastable structures of metals and alloys to be obtained. Moreover, because one avoids the effects of nucleation and growth on a specific substrate, one may tailor the properties of the films by choosing the appropriate preparation conditions of the preformed clusters.

Finally, several new routes to produce bulk nanocrystalline metals and alloys have been pursued. One example is based on friction stir processing to refine the grain sizes to a nanoscale. The method is limited to thin metal sheets that are processed in a multi-pass overlapping sequence. So

far, the method has been fairly successfully explored for Al alloys [50].

Readers are referred to the various papers cited above for further details concerning the processing of nc metals and alloys.

3. Mechanical properties derived from nanostructuring

This section outlines the considerable progress made over the past several years, from the perspective of the control of macroscopic (continuum) "materials response". The highlight is the improved and sometimes optimized mechanical properties achieved very recently by engineering the microstructure on the nanoscale in high-quality nc/ns metals. Behavior either newly contrasted against, or unusual relative to, coarser grained metals will be described. This is done for each of a comprehensive set of basic mechanical properties, including strength, ductility, strain rate and temperature dependence, fracture, fatigue and tribological wear resistance. Only fcc metals will be covered in this review, because they are the class of metals for which systematic data sets are available. It will become apparent that nc materials offer unprecedented mechanical properties, although, as noted above, there are issues related to structural stability. The nc or ns regime has also opened up new horizons in terms of fundamental understanding of deformation behavior and novel microstructural design. In addition, critical phenomena, such as stress-assisted grain growth and its effect on the deformation behavior of the nc materials, and critical behavior, such as the high sensitivity to strain rate of nc metals, will be discussed. Both of these aspects, among other nc properties, have been the subject of much recent experimental and theoretical interest.

3.1. Strength

Extraordinary mechanical strength can be derived through nanostructuring. This is an extrapolation of the well-known engineering practice of grain refinement for strength. The yield strength of polycrystalline metals is generally observed to increase as the grain size decreases according to the empirical Hall–Petch (H–P) relationship [51,52]:

$$\sigma_y = \sigma_0 + K_d d^{-1/2} \quad (1)$$

where d is the grain diameter, σ_y is the yield strength, and σ_0 and K_d are material dependent constants. A physical basis for this behavior is associated with the difficulty of dislocation movement across grain boundaries and stress concentration due to dislocation pile-up. Based on Eq. (1), metals with nanoscale grains should be much stronger than their coarse-grained counterparts.

Indeed, extremely high strength and hardness have been observed in nc metals, especially recently using high-quality nc samples. The strength and hardness have been found to increase with decreasing grain size [53]. For example, a summary of the hardness vs. $d^{-1/2}$ for Cu reported in the literature is presented in Fig. 1a. The hardness of nc Cu with an average grain size of 10 nm can be as high as 3 GPa, corresponding to a yield strength $\sigma_y \approx 1$ GPa, which is more than one order of magnitude higher than that of coarse-grained Cu ($\sigma_y \approx 50$ MPa). A similar plot is shown in Fig. 1b for the yield strength of various Cu specimens obtained from tensile tests [25,54–62]. Clearly, the measured hardness as well as the yield strength in Fig. 1 follow the traditional H–P relationship, even when the grain size is as small as 10 nm. Similar phenomena have been reported by Knapp and Follstaedt [63] for nc Ni and by Schuh et al. [64] in nc Ni–W alloys, where the H–P relationship remains valid when the grain sizes are as small as several nanometers. The mechanisms for the continued H–P strengthening down to $d \approx 10$ nm are not fully understood as yet, as the traditional picture of dislocation pile-ups is not expected to be applicable to nc grains. Models involving grain boundary processes lead to a d^{-1} dependence, as discussed in Section 4.

It has been argued that, when the grain size is extremely small, grain boundary processes could be enhanced to a level where they control plastic deformation. Therefore, one of the issues in debate has been whether the H–P relation breaks down at a critical grain size. In Fig. 1, there is no clear indication of such a critical grain size for copper at room temperature under ordinary strain rates. In computer simulations, Van Swygenhoven et al. [69] identified a criti-

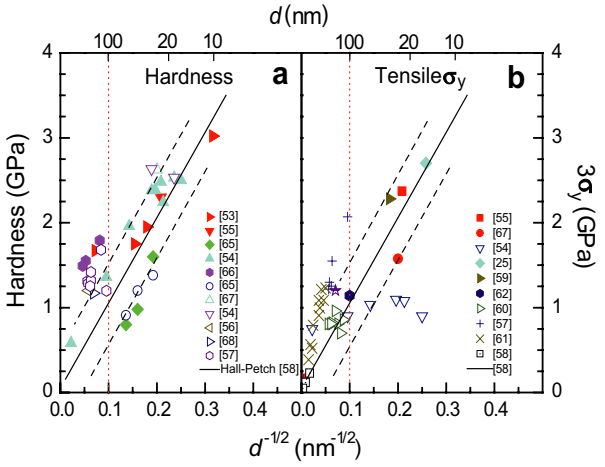

Fig. 1. (a) Summary of experimental data from the literature on the grain size dependence of strength of Cu specimens. The strength (or hardness) is plotted vs. $d^{-1/2}$. Literature data on hardness [53–55,65,66] (solid symbols) and yield strength (multiplied by 3) from compression tests [54,56,57,65,67,68] (empty symbols) are included in (a), and the literature data of tensile yield strength [25,54–62] are included in (b). The straight lines represent the H–P relation extrapolated from mc Cu [58]. Note that most ultrafine crystalline (ufc) Cu samples (with d in the submicron regime) exhibit higher hardness and tensile strength than the H–P expectation. The possible reason may be related with the fact that the ufc samples were prepared via severe plastic deformation, in which dense dislocation walls, tangles, cell walls or even subgrain boundaries are formed. These are barriers to the motion of dislocations and hence strengthen materials. (Figure taken from Ref. [53].)

cal grain size for Cu at about 8 nm: for grains smaller than 8 nm, the plastic deformation was dominated by GB sliding. Another molecular dynamics (MD) simulation study, by Schiøtz and Jacobsen [70], indicated that a maximum flow strength occurred in Cu at $d = 10$–15 nm, corresponding to a shift in the microscopic deformation mechanism from dislocation-mediated plasticity to GB sliding. Other recent models [71,72] propose that there can be a "strongest size" below which some grain boundary shear mechanism kicks in. However, such a maximum strength or hardness has not been fully confirmed experimentally (see again Fig. 1). Earlier experimental observations of the so-called inverse H–P relation in Cu had been attributed to sample defects, such as flaws, porosity or contamination [54]. One may thus conclude that grain size strengthening persists at least to a grain size on the order of 10 nm for Cu. Nanostructuring can indeed offer extremely high strength/hardness when such properties are needed for certain structural or coating applications. It is remarkable that a simple, relatively soft metal like Cu can be made to exhibit a strength as high as ~1 GPa through nanostructuring as shown in Fig. 1 (see also Sections 3.2 and 3.3). For $d \leqslant 10$ nm, softening may be possible, but this remains to be further validated experimentally, as fully dense nc bulk experimental samples with uniform grain sizes of less than 10 nm are very difficult to produce, although MD simulations [15,69,70,73], the bubble raft model [74] and limited experiments on nc Ni [22,75] have suggested that the critical grain size for decreasing strength may be on the order of 7–15 nm.

3.1.1. Strengthening using nano-twinned microstructures

While the use of general high-angle grain boundaries has been the focus for increasing strength in previous studies of nc materials, it has been recently demonstrated that nanoscale growth twins can be an effective alternative. Twin boundaries (TBs) not only are an effective barrier to dislocation motion and hence a potent strengthener [25], but also help retain ductility (see Section 3.2) and electrical conductivity. By introducing a high density of nanoscale growth twins, Lu and collaborators [25,76–79] demonstrated a significant size-dependence of mechanical properties on the twin lamellar spacing (λ), much like the grain size dependence of the strength in nc metals. This is demonstrated by the tensile stress–strain curves in Fig. 2a whereby, with decreasing twin lamellar spacing, both the tensile strength and the ductility increase remarkably. The series of Cu samples in Fig. 2a has a similar submicrometer average grain size (400–500 nm) but different twin densities. With increasing twin density, or decreasing twin lamellar spacing, the strength of the nano-twinned Cu (nt-Cu) sample increases gradually. The plot of yield strength as a function of $\lambda^{-1/2}$ of the nano-twinned Cu, in comparison with the H–P plot with $d^{-1/2}$, is shown in Fig. 2b. The agreement with the empirical H–P line suggests that the strengthening effect of TBs is analogous to that of conventional GBs in Cu, even when the twin spacing is decreased to the nanometer scale. For the nt-Cu sample with an average twin lamellar spacing of ~15 nm, the tensile yield strength, σ_y, reaches 900 MPa and the ultimate tensile strength 1068 MPa, which is similar to, or even larger than, those reported for polycrystalline pure Cu with three-dimensional nano-sized grains. Additional discussion of the effective blockage of dislocation motion by the numerous coherent TBs which act as strong obstacles is given in Section 4.2.5.

3.1.2. Strength reductions due to dynamic grain growth

During prolonged mechanical tests, or for samples that have very high purity, the high strength discussed above

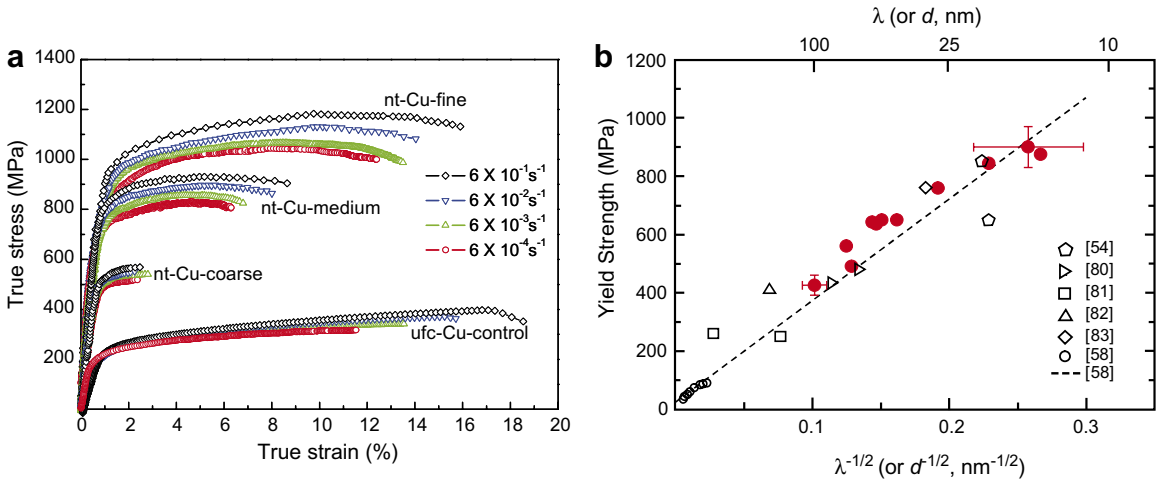

Fig. 2. (a) Tensile true stress–true strain curves for three different as-deposited Cu samples (nt-Cu-coarse, nt-Cu-medium and nt-Cu-fine: twin densities are 100 nm, 35 nm and 15 nm, respectively); for comparison, tensile stress–strain curves for a ufc-Cu-control sample without growth twins produced using the same electrodeposition solution are also included [25,76,78]. (Figure taken from Ref. [78].) (b) A plot of tensile yield strength as a function of the $\lambda^{-1/2}$ (where λ is the average lamellar spacing determined from statistic TEM observations) for the as-deposited nt-Cu samples [77] (solid circles). For comparison, H–P plots for the mc Cu [58] (straight line and open circles) and the nc Cu samples with various grain size are included [54,80–83]. (Figure taken from Ref. [77].)

may degrade with time. This is due, no doubt, to the large excess energy associated with grain boundaries in nc materials which is expected to cause instability in their nc grain size distributions. Evolution towards equilibrium can be driven, or promoted, by stress during deformation. Indeed, recent studies have found that indentation induced rapid grain growth in nc Cu [84,85] and nc Al [86]. For nc Cu samples, hardness drops significantly as the indenter dwell time increases. Grain growth was observed near the indented region during microhardness testing at both cryogenic and room temperatures. Surprisingly, it is found that grain coarsening is even faster at cryogenic temperatures than that at room temperature. Here it is also interesting to note the influence of impurities. Using in situ nanoindentation in a transmission electron microscope (TEM), extensive grain boundary motion has been observed in pure Al [86], whereas Mg solutes effectively pin high-angle grain boundaries in the Al–Mg alloy films [87]. The proposed mechanism for this pinning is a change in the atomic structure of the boundaries, aided by solute drag on extrinsic grain boundary dislocations. The mobility of low-angle boundaries is not affected by the presence of Mg.

After these initial observations of indentation-induced grain growth in IGC nc Cu and Al [84–86], grain growth was observed experimentally in nc materials that are deformed under other deformation modes; for example, high pressure torsion (HPT) processing-assisted grain growth in nc ED Ni [88], compression-induced grain growth in an nc Ni–Fe alloy [89], and even tensile deformation-assisted grain growth in nc Al [90] and nc Co alloy [91]. Recently, Zhu et al. [92,93] attempted to simulate the time evolution of the hardness considering grain size distribution so as to obtain a consistent explanation of the grain growth phenomena. More details of the simulation results will be reviewed in Section 4.2.4.

The fact that the grain growth process occurs at low temperatures raises the following critical questions. (1) What is the effect of stress-assisted grain growth on the comprehensive mechanical behavior during the plastic deformation? In addition to the decrease in hardness/strength discussed here, changes in ductility, fatigue behavior, etc., are also expected. (2) What is the effect of the initial microstructure of the nc materials, including grain size, grain size distribution [92,93], grain boundary energy, impurity content, defects and residual stress, on the grain growth process? (3) What is the critical condition (stress, strain, loading rate, etc.) required to induce grain growth in nc materials? (4) What are the atomic-level mechanisms for the mechanically driven, and perhaps diffusionless, grain growth? These critical issues are currently in debate and need to be further investigated.

3.2. Ductility and fracture

The ductility of a metal is usually defined as the ability to plastically deform without failure, via fracture, under tensile stress. In addition to ultrahigh strength, which is a desired and expected benefit of nanostructuring, reasonably good ductility (tensile elongation 10% or above) is another attribute that nc or ns metals are required to possess in order for them to be practically competitive as new structural materials. There has been exciting recent progress in developing nc metals that offer not only gigapascal strength but also good ductility, even for grain sizes as small as ~20 nm. We will devote extensive discussion below to the ductility issue, because a high ductility together with high strength is difficult to achieve.

Up until 2003, the literature data accumulated indicated that nearly all nc metals had tensile elongation to failure of no more than a few percent, even for those fcc materials that are very ductile in coarse-grained form [94–96]. Fig. 3 provides representative data for tensile elongation to failure vs. yield strength for nc metals [16,25,54,97–105]. It is evident that, in general, the ductility of high-strength nc/ns metals is much lower than their conventional microcrystalline (mc) counterparts. For example, mc Cu can have an elongation-to-failure as large as 60%, but the elongation-to-failure of most nc Cu samples (with $d \leqslant 25$ nm) is nowhere near such a value [95]. An exception is an electrodeposited Co sample ($d = 12$ nm) which exhibited a high strength (three times higher than mc Co) along with a reasonable ductility, viz. 7%, which is not much lower than conventional Co, at room temperature.

For many of the earlier nc materials, low ductility and premature fracture, sometimes failure occurring even in the elastic regime, were due to processing flaws and artifacts [13,59]. This was especially true when nc specimens were made by "two-step" processes that required a consolidation step. With these processes, artifact-free bulk samples are difficult to obtain. Large residual stresses, porosity, contamination from gaseous and metallic species as well as the imperfect bonding between particles are inev-

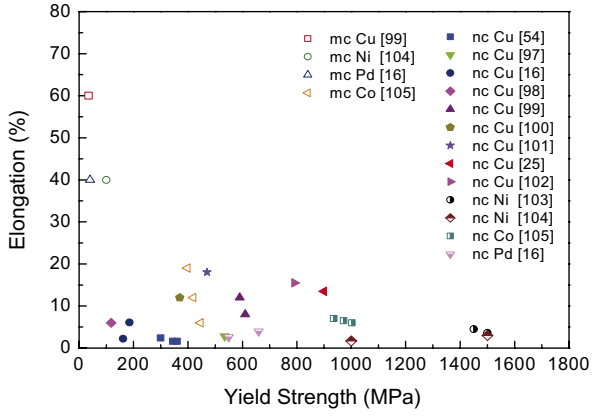

Fig. 3. Tensile elongation to failure of various nanocrystalline metals ($d \leqslant 100$ nm) in the literature [16,25,54,97–105] plotted against their yield strength. Note that most of the nanometals show a rather low ductility (≤10%). The data of nc Zn samples prepared by means of mechanical attrition [106] were not included in this figure, because Zn has a low melting point, and room temperature is at 0.42 of its melting temperature. It therefore may not be appropriate to compare it with the other materials in terms of deformation behavior at room temperature.

itable, even when the consolidated sample reached the theoretical density.

Fracture is a complex phenomenon of initiation, propagation and coalescence of voids or cracks. Failure at low levels of plastic strain is often due to plastic instability. Intensely localized inelastic strain may cause early crack formation in otherwise ductile metals. The typical fracture morphology of nc metals consists of a mixture of ductile dimples and shear regions. However, the dimple size, while much smaller than that of conventional polycrystalline metals, is several times larger than the grain size. Yin et al. [107] showed that the spacing and size of dimples are on the order of 1 μm, which is considerably larger than the grain size (19 nm) in the nc Ni they studied. The results of Kumar et al. [108] and Hasnaoui et al. [109] are in agreement with this observation. The shear regions are a direct consequence of the increased tendency of the nc metals to undergo shear localization. We note that shear localization is known to be promoted when the ratio of strain hardening rate to prevailing stress level falls below critical values [110]; since it is typically the case that such ratios are low in nc metals, it is expected that they may be prone to localized shear deformation [59,99].

Recently, Youssef et al. [102] reported flaw-free nc Cu made via a unique process of in situ consolidation through mechanical milling at both liquid nitrogen and room temperature. The Cu produced was reported to be artifact free, i.e. with no porosity, and minimal impurity contamination. The tensile true stress–strain curve for this bulk nc Cu is compared with that of the conventional Cu in Fig. 4. A very high yield strength (791 ± 12 MPa), along with 14% uniform elongation accompanied by obvious strain hardening and 15.5% elongation to failure, was observed. This ductility is much greater than that previously reported for all nc metals of similar grain size. Moreover, Li and Ebrahimi [111] reported that, without using electroplating additives that may degrade ductility, they could still electroplate metals and alloys with nanocrystalline grain sizes ($d = 44$ nm for Ni and 9 nm for an Ni–15%Fe alloy). Their Ni showed a tensile strength of ~1080 MPa, an elongation to failure of ~9%, a uniform ductility of 6–7%, and strong work hardening. The Ni–15%Fe displayed an impressive tensile strength of over 2300 MPa, an elongation to failure of ~6%, a uniform ductility of 4–5% and very strong work hardening. Erb et al. [112] recently also tested Ni–Fe alloys prepared using electrodeposition. Ductility similar to, or even better than, that reported by Li and Ebrahimi [111] was also observed. They attributed the ductility to the relatively large thickness of their new samples that better met the ASTM standards; their new samples were now millimeters thick, whereas those tested earlier were much thinner than 1 mm. Very thin samples may be susceptible to instability and premature failure because of, for example, their increased sensitivity to the propagation of small surface cracks. In any case, it appears that after minimizing processing artifacts, nc metals can indeed be made very strong and ductile. Such a discovery, along with further optimization of processing and properties, can have major implications for the application of nc metals as structural materials.

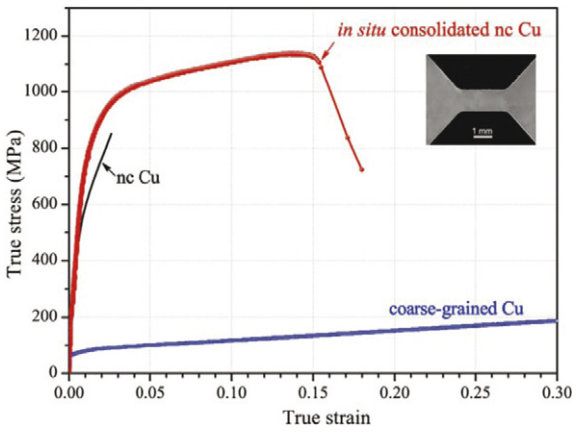

Fig. 4. A typical tensile true stress vs. strain curve for a bulk in situ consolidated nanocrystalline Cu sample (with an average grain size of 23 nm) with high purity and high density in comparison with that of coarse-grained polycrystalline Cu sample (with an average grain size larger than 80 μm) and a nanocrystalline Cu sample (with a mean grain size of 26 nm), prepared by an inert-gas consolidation and compaction techniques. (Figure reprinted with permission from *Applied Physics Letters* 2005;87(9):091904. Copyright 2005, American Institute of Physics.)

A major factor limiting the uniform tensile elongation is the tendency for plastic instability, such as shear band formation or necking. Localized deformation modes such as these may occur in the early stages of plastic deformation due to the decreased strain hardening capacity, whereas a reasonably high strain hardening rate is required to stabilize the tensile deformation at stress levels that prevail in high-strength nc metals [10,59]. The strain hardening capacity of nc metals is not expected to be very large as their extremely small grain size makes it difficult to store dislocations. Indeed, the conventional mechanism for the high work-hardening rates in fcc metals, including the formation of dislocation locks, formation of dipoles and significant pinning due to dislocation intersections, have yet to be experimentally confirmed for nc materials during room-temperature tensile tests [102]. It is expected that any improvements of the strain hardening will be beneficial to enhancing the homogeneous plastic deformation for nc materials. Significant strain hardening is seen in the high-strength, high-ductility Cu in Fig. 4. This is in contrast to all previous nc metals, which showed appreciable strain hardening rates only during the initial stage of plastic deformation, i.e. over the initial couple of percent of plastic strain. In this context, one could interpret the success in Fig. 4, and the other cases cited above, as follows: the high-quality samples recently developed allowed one to take advantage of the intrinsic work hardening capability of the nanocrystalline grain structure in certain cases. The exact mechanisms for such strain hardening sustainable over a range of strains, however, require future study, since it is unlikely that the hardening comes only from the conventional dislocation storage mechanism [102,111],

given the tiny grains that encourage dynamic recovery during room-temperature deformation [59].

An appropriate grain size distribution could also impart both high strength and ductility [113,114]. This approach has been demonstrated for Cu [114] through an intentionally designed bimodal distribution realized via recrystallization and secondary recrystallization, in consolidated Al alloys made of powders with different grain sizes [115] and other materials [116]. A grain size distribution can also result from stress-assisted grain growth, developed in situ during (tensile) testing [90]. As mentioned in the discussion on dynamic grain growth [84–86,90], this occurs because nc metals have grain sizes so small that there is a large driving force for grain growth, and the applied stresses during plastic flow can be very high. In addition, nanocrystalline grains are often prepared via vapor deposition/condensation. In such processing the content of impurities that could pin the grain boundaries can be kept quite low. The coarsened grain structure can be bimodal due to the abnormal growth mode, or exhibit a wide grain size distribution. Tensile ductility was found for otherwise brittle nanocrystalline thin films, e.g. in vapor-deposited Al [90]. In all these cases, strain hardening was improved because of the mechanisms made possible by the inhomogeneous grain structure [10]. More discussion with respect to mechanisms and the role of grain size distribution will be presented in Section 4.

It is interesting to note that the twin boundary strengthening strategy discussed in Section 3.1 (Fig. 2a), while imparting high strength, can retain an adequate strain hardening rate in the nanostructure. In fact, elongation-to-failure for the nano-twinned Cu in Fig. 2a increases considerably with increasing twin boundary density. The Cu sample with the highest twin density shows both high strength and ductility, as illustrated in Fig. 2a. It is proposed that high densities of dislocations could be accumulated near the regions of TB and facilitate uniform plastic deformation [117]. Meanwhile, nano-twinned Cu has multimodal distributions of length scales, which is known to benefit ductility [83]. The twins subdivide the submicron-sized grains into nanometer-sized twin/matrix lamellar structures, of which the length scale parallel to the TBs (plastically soft direction) is of the order of submicrometers, whereas that in the direction transverse to TBs (the plastically hard direction) is at the nanometer scale [78]. In the former direction, dislocation glide/accumulation is relatively easier, while it is more difficult in the latter direction. This suggests that the nanostructuring strategy of using high density nanoscale coherent twin boundaries to "replace" the more typical general high-angle nanocrystalline grain boundaries can also lead to a combination of high strength and high ductility for pure nc metals [117].

When nanoscale structures are used as the base system into which other microstructural features are introduced, including grains or twins of varying length scales, second phase particles, deformation-induced phases and grain boundaries of nonequilibrium nature, the ductility and strength of nc/ns materials can be improved and optimized via a number of ways [10]. These approaches often involve microstructures in the ufc regime, i.e. at scales above 100 nm, and hence are not covered in detail in this overview.

3.3. Strain rate and temperature dependence of strength

The strain rate and temperature dependence of the strength and ductility of nc metals will be summarized in this subsection. This dependence has been found to be rather strong in nc or ns metals, more so than had been realized previously. The engineering parameter measuring strain-rate sensitivity, m, is commonly defined as

$$m = \frac{\partial \log \sigma}{\partial \log \dot{\epsilon}}\Big|_{\epsilon,T} \tag{2}$$

where σ is the flow stress and $\dot{\epsilon}$ the corresponding strain rate. The exponent m, in a $\sigma \propto \dot{\epsilon}^m$-type relation, is one of the key engineering parameters for controlling and understanding the deformation in metals. For example, a highly strain rate sensitive material is expected to resist localized deformation and hence be ductile, and in the extreme case of very high rate sensitivity, be superplastic. Recent experiments have probed the strain-rate sensitivity of ultrafine grained and nanocrystalline metals, and revealed obvious and interesting differences from the behavior known for conventional metals. With decreasing grain size, an increase in m has been found to be common for fcc metals. For the behavior of bcc materials, the reader is referred to Refs. [9,118].

For nc Ni, Schwaiger et al. [103] systematically changed the loading rate and strain rate during controlled indentation of electrodeposited nc Ni (average grain size ~40 nm) and showed that the flow stress of nc samples was highly sensitive to the rate of deformation. Their results are reproduced in Fig. 5a. Dalla Torre et al. [119] and Wang et al. [120] found a similar tendency for nc Ni samples by means of tensile tests, including jump tests and relaxation experiments (see Fig. 5b).

Fig. 6a summarizes the variation of m as a function of grain size, d, for Cu samples, based on literature data [53,56,121–126]. The variation of m vs. twin lamellar spacing, λ, is also included (with open symbols) for comparison [76]. Despite some inconsistencies in the absolute values obtained from different research groups or those arising from different sample synthesis methods and different testing methods, there is a consistent and clear trend: the m value increases with a decrease of grain size from the micron to the submicrometer scale (m from 0.006 to about 0.02), followed by an obvious "take-off" when the grain sizes are reduced to below a couple of hundred nanometers. In the nanoscale regime, m is much larger than that reported for conventional Cu. The current suggestion is that the highly localized dislocation activity (e.g. dislocation nucleation and/or dislocation de-pinning) at the GBs

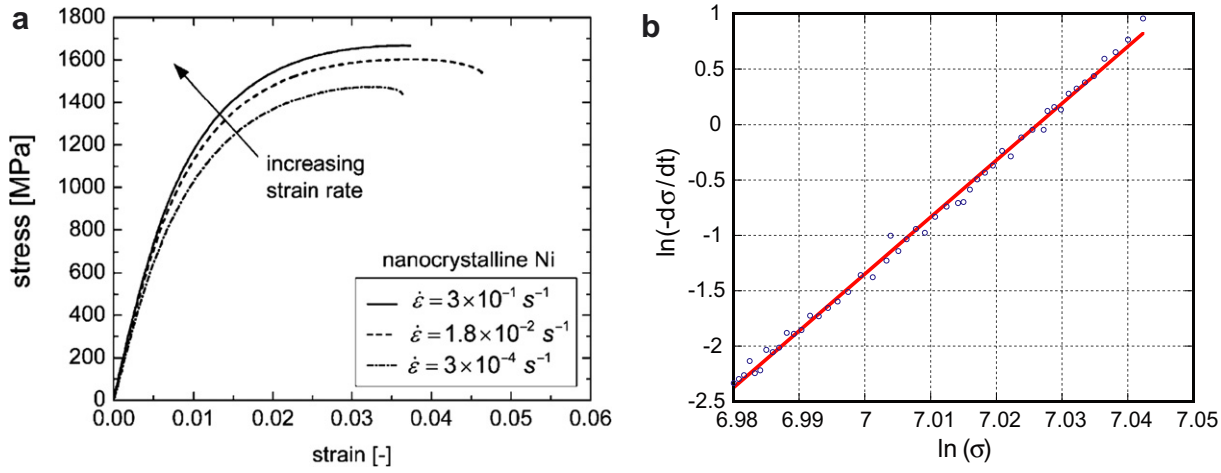

Fig. 5. (a) Engineering stress–strain curves of an electrodeposited nanocrystalline Ni with an average grain size of 40 nm, obtained from tensile tests at different strain rates. (Figure taken from Ref. [103].) (b) Plot to determine strain rate sensitivity using Eq. (2), from stress change rate data obtained in a stress relaxation test at room temperature, for nc Ni (average grain size $\sim$ 30 nm). The strain-rate sensitivity is obtained from the slope of the linear fit, $m = 0.02$. (Figure taken from Ref. [120].)

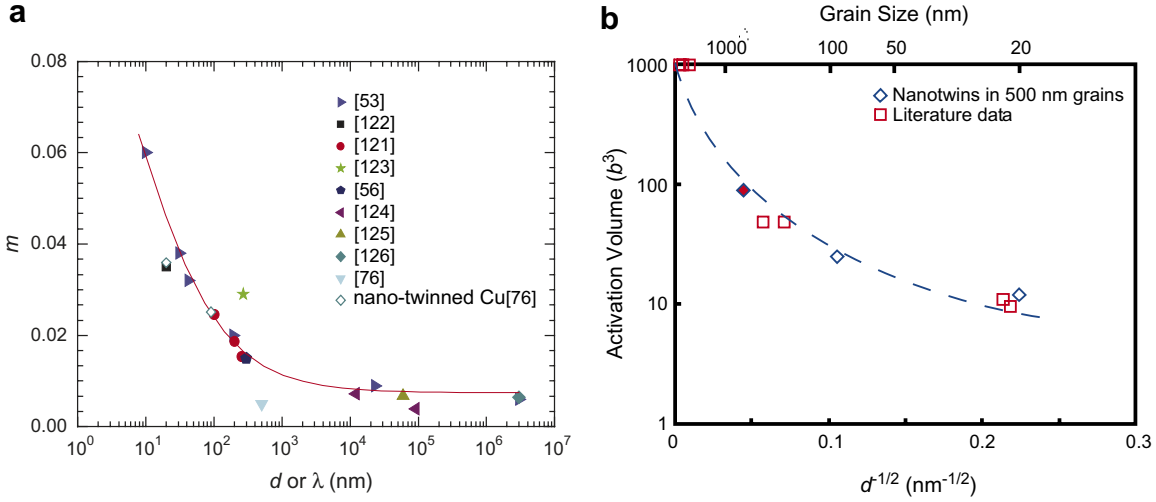

Fig. 6. (a) Summary of the room temperature strain rate sensitivity m, as a function of grain size, d, for Cu from the literature [53,56,121–126]. Note that this figure includes data not only for nanocrystalline Cu but also for the ultrafine- and coarse grained reference to cover the entire range of d. The variation of m vs. twin lamellar spacing, λ, is also included (with open symbols) for comparison [76]. There is a clear trend for m to significantly increase with decreases in the characteristic length scale, i.e. grain size or twin lamellar spacing. (b) A plot (figure taken from Ref. [127]) of the effect of grain size on the activation volume, measured in units of b^3, for pure Cu and Ni from available information. Also indicated are two data points, denoted by open diamonds, corresponding to the same set of experiments for which m values shown in (a), for pure Cu with nanoscale twins were taken [76]. For these cases, the twin spacing is plotted instead of the grain size.

leads to an enhanced strain-rate sensitivity for nc metals [103,120,121,127,128]. Fig. 6b shows a plot of the effect of grain size on the activation volume [127], measured in units of b^3, for pure Cu and Ni, and where b is the magnitude of a perfect dislocation.

The overall strain-rate dependence of a material is influenced by dislocation activity, GB diffusion, and lattice diffusion [99,129–132]. Generally the contribution of lattice diffusion is negligible at room temperature. For mc fcc metals, the rate-controlling process is the cutting of forest dislocations, resulting in a low strain-rate sensitivity. With d decreasing into submicrometer and nc regimes, forest cutting mechanisms subside as now it is the large number of GBs and/or subgrain boundaries that serve as obstacles to dislocation motion. The rate-limiting process is increasingly influenced by dislocation–GB interactions. Cheng et al. [99] recently presented a summary of strain-rate sensitivity as a function of grain size, down to grain sizes of 20 nm. They explained the elevated strain-rate sensitivity by using a model considering the length scales in nc grains during grain boundary–dislocation interaction. More comments on the underlying mechanisms will be presented in Section 4, where the origin of the small activation volume is discussed.

Although the m value of Cu is enhanced by an order of magnitude when the grain size is reduced to about 10 nm, the largest m value observed (0.06) is still much smaller than that expected for the plastic deformation process controlled by GB sliding ($m = 0.5$) [133] or Coble creep ($m = 1.0$) [134]. Taken as a whole, the results indicate that grain boundary diffusion-mediated mechanisms are not yet dominant over dislocation-based processes for grain sizes down to 10 nm. This is consistent with observations that the hardness in Cu increases with decreasing grain size down to 10 nm, still following the classic H–P relation.

An increased strain-rate sensitivity was also observed in ultrafine grained Cu with a high density of coherent twin boundaries (CTBs). The loading rate sensitivity of Cu with a twin lamellar spacing of 20 nm was shown to be 0.035, about seven times higher than that of ufc Cu without twins [76]. With a decrease of TB density, m also decreases. The dependence of m on the twin lamellar spacing has been included in Fig. 6a. The authors suggested that the CTBs in the nt-Cu specimen serve as barriers for dislocation motion and sources for dislocation nucleation, much like the general high-angle GBs. The highly localized dislocations in the vicinity of TBs, as indicated by TEM images [76–78], appear to lead to an enhanced strain-rate sensitivity.

There have been indications that the elevated strain rate sensitivity index m in nc/ns metals plays a role in improving strength/ductility properties. The strength increase due to the rate sensitivity is seen in Fig. 5a. Valiev et al. [62] attributed the large ductility observed for an nc Cu sample after 16 passes of equal channel angular extrusion (grain size 100 nm) to an unusually large m of 0.14. Wang and Ma [114] argued that the moderately elevated m could delay necking to a plastic strain of the order of 10% due to the strain rate hardening mechanism. Champion et al. [135] observed nearly perfect plastic behavior in the absence of strain hardening in an nc Cu (grain size reported to be 80 nm) prepared via consolidation. The uniform tensile deformation to about 12% plastic strain may also be due to the stabilizing effect of an enhanced value of m [114].

Corresponding to the enhanced strain-rate dependence, there is also a more pronounced temperature dependence, arising from the thermally activated deformation mechanisms controlling the plastic flow. A rapid increase in yield strength has been documented for nc Ni and Cu, when the deformation temperature is lowered to below room temperature [136]. This feature could be useful for cryogenic applications. The origin of the strong temperature dependence, as well as for the rate sensitivity, has been linked to the small activation volume of dislocation mobility observed in strain rate change tests [120,121,127,136,137]. The activation volume, in turn, is a signature of the underlying deformation processes [127]. Three specific interaction scenarios have been discussed by Asaro and Suresh [127], Wang et al. [120,136] and Van Swygenhoven et al. [128,137]. More discussion will be presented in Section 4.

3.4. Fatigue

Grain refinement has long been a possible strategy to improve fatigue and fracture resistance of engineering metals and alloys [138]. Many studies in the literature have dealt with mc materials [138]. Limited data are available for ufc materials, processed mostly via equal channel angular pressing (ECAP) methods [139–142]. Only a few studies [141,142] have been conducted so far on nc materials.

In the mc and ufc regimes, grain refinement was found to result in the following two trends: (1) higher fatigue endurance limit caused by the elevated strength due to grain refinement; and (2) deteriorated fatigue damage tolerance, especially in the low stress intensity range [141,142]. The fatigue fracture resistance was considered to be related to the possible microstructure-driven crack path changes due to the grain size changes [143].

It is of great interest to study the effects of grain refinement on fatigue behavior at the nanoscale range when average, as well as peak, grain sizes are all below 100 nm. Witney et al. [144] studied IGC nc Cu samples with a density of 97.4–99.3%. The maximum stress amplitudes ranged from 50% to 80% of the yield stress, and the minimum stress was 10 MPa. After several hundred thousand cycles, a moderate increase in grain size was observed (on the order of 30%). The cyclic deformation in their tests appeared to be elastic.

To date, there is but a single set of published reports [141,142] on the fatigue life and fatigue crack growth for full-density nc metals. Using electrodeposited nc Ni (with an average grain size in the range 20–40 nm, and peak grain size near 70 nm), Hanlon et al. [141] showed the effect of grain size on the fatigue resistance of initially smooth-surfaced pure Ni (see Fig. 7a) in terms of S–N curves. Nanocrystalline Ni was shown to have a moderately higher endurance limit when subject to stress controlled fatigue loading than ufc Ni, while both nc Ni and ufc Ni showed significantly higher fatigue resistance than the mc Ni. On the other hand, systematic follow-up work [142] confirmed that over a wide range of load ratios nc Ni showed significantly lower resistance to fatigue crack growth. A summary plot can be found in Fig. 7b where the stress intensity factor range ΔK required for a growth rate of 10^{-6} mm/cycle in ufc and nc Ni is plotted as a function of maximum stress intensity factor K_{max}.

To understand the mechanism of crack growth vs. grain refinement, the previous model proposed by Suresh [143] can be used. The model suggested that predominantly crystallographic and stage I crack growth result in microstructurally tortuous crack paths in coarser grained materials. Fig. 8 shows SEM crack growth images of mc, ufc and nc Ni subjected to fatigue loading at 10 Hz and loading ratio $R = 0.3$. The crack path is much less tortuous with an decreasing grain size. Using the quantitative model found in Ref. [143], the predicted results match fairly well with the experimental data sets at different grain sizes and R values [142].

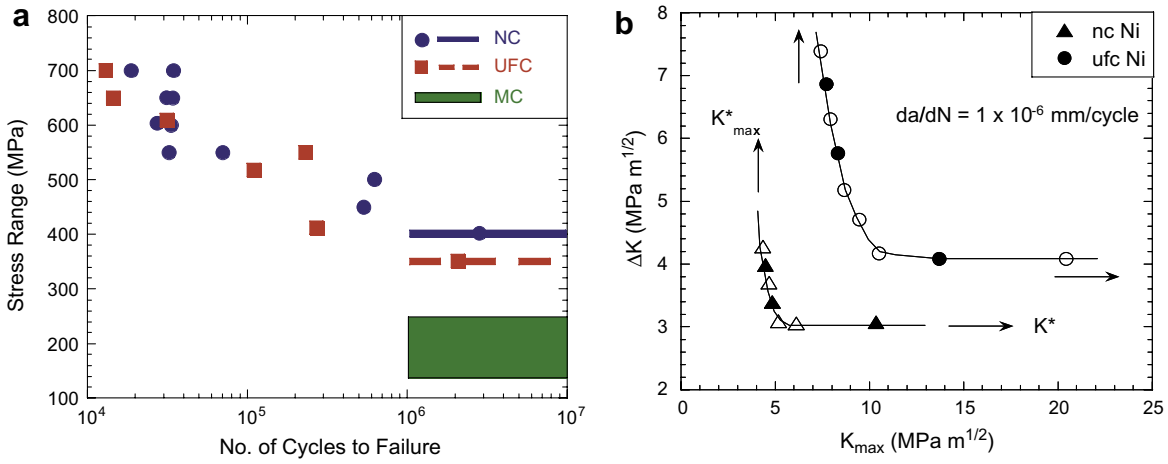

Fig. 7. (a) The effect of grain size from the micro- to the nano-regime on the cyclic stress vs. total number of cycles to failure plot in pure Ni. (Figure reprinted from Ref. [141]. Copyright 2003, with permission from Elsevier.) (b) Stress intensity factor range, ΔK, required for a growth rate of 10^{-6} mm/cycle in ufc and nc Ni plotted as a function of the maximum stress intensity factor K_{max}. ΔK and K_{max} denote the limiting, or threshold, values of alternating and maximum values of stress intensity factor required for the particular crack growth rate of 10^{-6} mm/cycle. The detrimental effect of grain refinement at the nanoscale on crack growth is apparent in the figure. (Figure reprinted from Ref. [142]. Copyright 2005, with permission from Elsevier.)

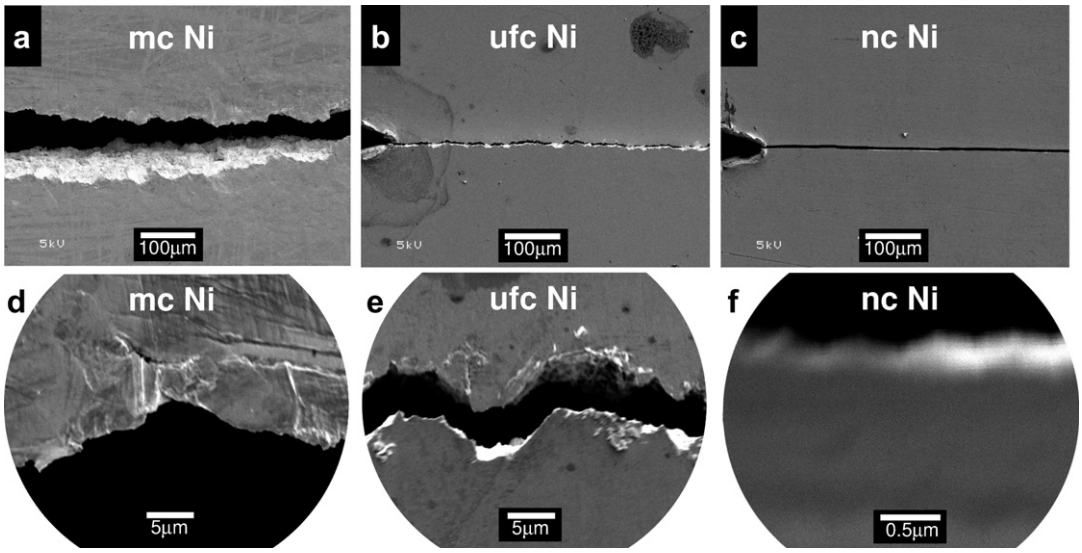

Fig. 8. Scanning electron micrographs of mc, ufc and nc Ni subjected to sinusoidal fatigue loading at initial ΔK values of 10, 6.2, and 8.5 MPa $m^{1/2}$, respectively. A cyclic frequency of 10 Hz and loading ratio $R = 0.3$ were used in all cases. Crack path tortuosity clearly decreases with grain refinement. Images (d)–(f) are high-magnification images of (a)–(c), respectively, and the magnification of (f) is 10 times that of (d) and (e). (Figure reprinted from Ref. [142]. Copyright 2005, with permission from Elsevier.)

With the enhanced fatigue limit for nc metals but the reduced crack growth resistance, it is likely that a controlled grain size gradient may bring beneficial fatigue properties while avoiding unwanted disadvantages. In fact, the idea of surface treatment to get nanocrystallized layer on the surface was successfully explored [145,146]. An MD model simulating fatigue crack growth at the nanoscale [147] showed that the fatigue crack growth mechanism involves dislocations emitted from the crack tip and nanovoids formed ahead of the main crack. The predicted crack growth rates as a function of stress intensity amplitude by Farkas et al. [147] are consistent with the experimental results reported in Refs. [141,142].

3.5. Tribological properties

Systematic studies of wear in pure nc metals are less common because of the difficulty in synthesizing bulk nc samples suitable for friction and wear tests. Recently, Han et al. [148] compared the dry sliding tribological behavior of an electrodeposited nc Cu and a conventional mc Cu. Experimental results showed that the wear resistance of nc Cu was enhanced. The steady-state friction coefficient of the nc Cu was obviously lower than that of the mc Cu when the load was below 20 N. The wear volume of the nc Cu was always lower than that of the mc Cu for the applied load ranging from 5 to 40 N. The difference

in wear resistance between the nc and the mc Cu decreased with increasing load. The enhancement of the wear properties of the nc Cu was associated with the high hardness and the low work-hardening rate of the nanocrystalline structure, and easy oxidation of wear debris, which are all related to grain refinement. Similar findings were reported by Bellemare et al. [149], who established a quantitative framework to evaluate frictional sliding.

Although, for some time now, hardness (H) has been regarded as a primary material property affecting wear resistance, the H/E ratio (E being Young's modulus), which is related to the elastic strain to failure, is a more suitable parameter for predicting wear resistance [150]. Within a linear-elastic approach, this is understandable keeping in mind that the yield stress of contact is proportional to (H^3/E^2) and that the critical energy release rate is proportional to σ_c^2 with σ_c the critical stress of fracture. As such, H^3/E^2 is a strong indicator of resistance to plastic deformation in loaded contact and the H/E ratio is an indicator of "elastic strain to failure" (and resilience). These rather simple considerations suggest that the fracture toughness of nanostructured material would be improved by both a low elastic modulus and a high critical stress for fracture implying also a need for high hardness. Therefore the best choice is not to focus on mono-component nc metal systems but rather to synthesize a nanocomposite material where nanocrystalline hard-metallic- or non-metallic particles are embedded in a relatively compliant metallic matrix. The advantage is that a nanocomposite material contains a high density of interphase interfaces that may assist in crack deflection and termination of crack growth [32,151,152]. Moreover, other mechanisms, like interface diffusion [153] and sliding [73,154,155], are also suggested to further improve ductility in nc multiphase structures. These findings could be expanded to the field of hard wear-resistant coatings to introduce ductility and prevent fracture under a high contact load, leading to super toughness [156]. Although mechanical properties, such as Young's modulus and hardness, of nanocomposite materials have been reported in some detail, only scant information is available on the correlation between the nanostructure, the mechanical properties and the macroscopic tribological characteristics [157]. In particular, amorphous carbon- or amorphous hydrocarbon-based nanocomposite coatings are expected to exhibit not only excellent wear resistance but also low friction due to the self-lubrication effects of the diamond-like carbon matrix, which make them environmentally attractive because liquid lubricants can be omitted [158–161].

Here some interesting results are briefly mentioned, in particular the example of nano-sized Cr particles embedded in a Cu matrix [162]. The overall conclusion is that binary alloys of a "nitride-forming" transition metal with another low-modulus, low-miscibility transition metal element appear to provide a promising route to achieve a high H/E ratio. The transition metal particle can be "doped" to supersaturation with an interstitial element (B, C, N or O) to increase yield strength. In addition, alloys made of mixtures of elements with different atomic radii and/or valence electron configurations provide challenges and opportunities to form a glassy metal film over a wide range of compositions. Like metallic nanocomposite materials, these glassy films provide hardness values in excess of 20 GPa, whilst retaining the (low) elastic moduli of the constituent metallic phases. Current work in this area is directed towards the introduction of crystalline nanometallic phases to "delocalize" shear band formation so as to enhance the H/E ratio [163,164].

By controlling the size and volume fraction of nc phases, the properties of the nanocomposite coatings can be tailored within a wide range, making a balance between hardness and elastic modulus, to permit a close match to the elastic modulus of the selected substrate. In such a way, a high toughness can be attained, which is crucial for applications under high loading contact and surface fatigue.

3.6. Outstanding issues

The central message of Section 3 is that recent research has established a group of nc or ns metals that exhibit extraordinary mechanical properties. They have impressive strength at least a factor of five higher than their conventional coarse-grained counterparts. Meanwhile, they possess considerable ductility in tension. The resistance to fracture, certain fatigue properties, wear resistance, etc., are found superior to coarse-grained metals. This is, obviously, cause for optimism: ultrahigh strength nc/ns metals are becoming practically useful for structural applications, if the processing barriers (such as throughput and the production cost) can be overcome.

However, there are also many outstanding questions remaining to be answered. The effective measures developed so far to improve and optimize mechanical properties of nc metals have not yet been fully understood. More in-depth quantitative analyses are clearly needed. What the findings summarized above do provide are useful ideas and hints for future developments in this field. These will lead to ample research opportunities. First, it remains to be seen how universal the observed effects of sample quality would be on strength, ductility and fatigue properties. The same question can be asked about the effects of nanoscale twins. Second, only a few model fcc metals, notably Cu and Ni, have been investigated in any detail. Metals of other crystal structures (e.g. bcc, hcp) have been explored to a far lesser degree, let alone nc/ns alloys that would be more useful in engineering applications. Third, several intriguing responses, different from coarse-grained metals, such as the stronger strain rate and temperature dependence, the localized deformation modes such as shear banding [118,165], and the work hardening behavior of nc materials, require systematic studies to firmly establish their origins. Fourth, it remains a challenge to synthesize samples with extremely small and yet uniform grain sizes on the order a few nanometers to unequivocally establish

the onset of the inverse H–P relationship and perhaps grain boundary sliding-mediated superplasticity. Fifth, it is important to experimentally track the detailed fracture initiation and growth in bulk nc materials. Sixth, various ways to improve fatigue properties of nc materials need to be explored, such as how plastic strength gradient (caused by modulating grain size distribution) would influence/benefit fatigue performance, etc. Finally, we point to the need to fully understand the phenomenon of grain growth during deformation and how to control it. The possibility of unstable nanostructures will undoubtedly discourage their practical use.

Clearly, the mechanical behavior observed has to do with the unusual deformation mechanisms operative in the nanoscale grains. This is covered in the following section.

4. Nanocrystalline deformation mechanisms and mechanisms-based constitutive modeling

As pointed out above, an understanding of the deformation mechanisms is important for understanding, controlling and optimizing the mechanical properties of nc metals. A number of questions immediately come to mind when examining the properties achieved in nc metals. For example, why do we observe the extremely high strength and a H–P strengthening down to grain sizes on the order of 10 nm? The concept of dislocation-mediated deformation has been cited many times in Section 3 within the discussion of properties. What, then, is the evidence of dislocation activity inside the grains and in the vicinity of GBs? If the deformation is indeed controlled by dislocations, what is it that differs from what we already know happens in coarse grains? In other words, what are the differences in the dislocation behavior from the normal mechanisms controlled by the intra-grain dislocation sources? Are the dislocations nucleated at grain boundaries? Is twinning a possible deformation mechanism in nanoscale grains? How is strain hardening possible in tiny grains and within their aggregates? How can we effectively mitigate localized deformation in nc materials? Why would the flow stress of nc metals exhibit an obvious strain rate and temperature dependence? What would the nanoscale grain size do to the fracture and fatigue properties of nc materials?

In the following, we present an update of the results from recent studies aimed at uncovering the deformation mechanisms and providing some clues to the questions posed above. We will not attempt to review recent literature in detail. Instead, we will highlight a few recent advances in understanding critical issues related to nc deformation mechanisms. Our emphasis is that it is now possible to develop mechanisms based constitutive laws for nc materials to directly compare with experimental results.

MD simulation results had been very helpful in identifying possible deformation mechanisms. Related MD studies will be cited throughout the text. However, due to the length limit of the current overview, the readers are referred to recent comprehensive discussions and reviews available in the literature [15,166] and the references cited therein for a comprehensive understanding on the merits and limitations of MD studies.

4.1. TEM studies on deformation mechanisms of nanocrystalline metals

Ex situ TEM observations were made on deformed Ni specimens with an average grain size of approximately 30 nm [108], following compression, rolling and nanoindentation. Isolated dislocations and evidence of sporadic dislocation networks within the larger grains were identified. However, the density of dislocations left in the specimens could not account for the high levels of imposed plastic strain. For the small nc grains, very few dislocations were found left inside the grain interior [108]. This lack of deformation debris is consistent with the findings of an in situ X-ray diffraction (XRD) experiment: upon loading, peak broadening was observed for the nc Ni sample, but the peak broadening was fully recovered upon unloading [167]. These results point to the absence of dislocation storage after room-temperature deformation. Other TEM work in many post-deformation nc specimens reached similar conclusions [97,168,169]. So where did the dislocations go if they are the dominant carriers of plasticity? MD simulations suggest that, after coming out of one side of the grain and traversing the grain, the dislocations usually disappear into the GBs on the opposing side, such that no debris is left [15,166]. Moreover, an individual dislocation that stops in the grain interiors might be expected to relax into nearby grain boundaries when the stress is removed. This picture also explains the lack of residual peak broadening in XRD measurements after the load is removed [167]. Therefore, in order to confirm the existence of dislocation activity during the deformation, it is useful to record the deformation process as it occurs, by recourse to an in situ TEM observation.

The first in situ investigation was performed on nc Au films by Ke et al. [170]. They found evidence of grain rotation, but not for dislocation activity at the 10 nm grain size. In contrast, at larger grain sizes, e.g. $d = 110$ nm, significant dislocation activity occurred and fracture was transgranular. During in situ TEM tensile testing, Hugo et al. [168] and Kumar et al. [108] obtained evidence for "pervasive dislocation nucleation and motion" in nc Ni, in grains as small as 10 nm, and Youngdahl et al. [171] reported evidence for dislocation pile-ups at grain boundaries in nc Cu with grain sizes down to 30 nm. The above reports suggested that grain boundary sliding or grain rotation might also have contributed to the overall plastic deformation, but no direct evidence, e.g. in the form of imaging of these mechanisms, were provided in their papers. More recently, Shan et al. [172] reported an in situ straining TEM observation of grain rotation in an nc Ni film with an average

grain size of 10 nm. Successive video frames in dark field TEM mode suggested that plastic deformation of nc Ni is mediated by grain rotation.

There are problems and uncertainties, however, associated with the interpretation of the results from these in situ TEM experiments. First, the rapid changes in diffraction contrast in nc grains, which have been interpreted as due to dislocation movements upon straining, can arise from other sources. Second, the Burgers vectors were not identified for dislocations because of the difficulties associated with in situ TEM experiments. Third, it must be noted that in such ultrathin TEM foils the observations are made in regions with highly non-uniform deformation right at the tip of an advancing crack. Fourth, in the ultrathin foil when only a few grains are sitting atop each other, dislocation activities, diffusion processes and changes in the grain boundary structures may have been enhanced due to inevitable free surface effects and the accelerated diffusive events near the surface under the electron beam. It is thus questionable if the in situ observations can faithfully represent bulk deformation behavior of the three-dimensional nc materials.

Recently, new TEM experiments have been designed to capture dislocations. This was done by taking high-resolution pictures during the relaxation of the in situ TEM foil before unloading, so that dislocations are trapped inside the grains by the applied stresses [172]. The alternative is to examine the grains after tensile deformation at liquid nitrogen temperature. The low temperature for deformation was employed not only to suppress possible grain growth assisted by stress during deformation, but also to retain some of the dislocations for postmortem TEM examination. Dislocation configurations of several types have been reported [169]. Since the dislocations are stored inside the grains only at liquid nitrogen temperature but not at room temperature, this indicates that the propagation, or de-pinning, of dislocations is a thermally activated process, in agreement with MD simulation [128] and XRD [173] results. The experimental identification of Burgers vectors and dislocation characters offer proof for the general belief that full dislocations do operate during deformation of the nanograins. A set of high-resolution TEM (HRTEM) images showing dislocations is shown in Fig. 9.

The formation of deformation twins and stacking faults, indicating the operation of partial dislocation mediated processes, has been considered as a contributing deformation mechanism [174–180]. This is based on recent TEM observations in Al [175–177], Cu [174], Pd [174,178], Ta [179] and Ni [180], as well as on analysis of dislocation processes as described below. However, almost all of the experimental evidence has been obtained in nc metals that were subjected to complicated stress states and high stress levels, such as occurs during indentation [175], grinding [175], high-pressure torsion [174], high-rate cold rolling [174,178], ball milling (sometimes with powders immersed in liquid nitrogen) [176,177] and SMAT [180]. Very recently, it was observed that the partial-dislocation mediated processes do occur during uniaxial tension, but only when the tests are carried out at liquid nitrogen temperature where high flow stresses are involved. Experiments have been performed on nc Ni, for which little defect accumulation is found at room temperature [169,181]. This is clear evidence of the dependence of deformation mechanisms not only on the nanocrystalline grain size but also on deformation conditions such as temperature. Such information is especially valuable for attempts to construct deformation maps for nc materials [182], which require a complete set of information regarding the effects of grain size, temperature and strain rate, as well as for the development of mechanisms based models.

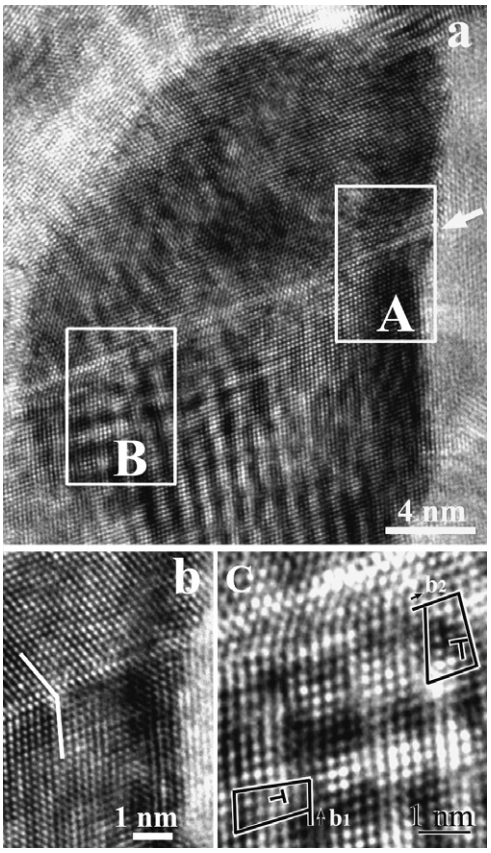

Fig. 9. (a) HRTEM micrograph of an nc Ni grain after tensile testing at liquid nitrogen temperature. A twin boundary is indicated by an arrow. (b) High magnification of the white-framed region A in (a) showing the details of the twin. (c) High-magnification view of the white-framed region B in (a) showing the presence of several full dislocations near the twin boundary and grain boundary. The Burgers circuits were drawn to identify Burgers vectors: $b_1 = 1/2[011]$ and $b_2 = 1/2[10\bar{1}]$. (Figure reprinted with permission from *Applied Physics Letters* 2006;88(23):231911. Copyright 2006, American Institute of Physics.)

The observation of deformation twins in very fine grains, where the twinning stress required is expected to be large (such as under MD simulation conditions [182]), has generated much interest and debate. It is especially intriguing that the deformation twins were first observed in nc metals with high stacking fault energy, such as Al [175,177,183]. A few ideas and models have been put forward to explain the observations [6,127,175,177,184]. MD

simulations have emphasized the importance of examining the generalized planar fault energy curves in understanding the selection of a particular process (full dislocations vs. stacking faults vs. twin nucleation) in a particular metal [185–187].

4.2. Mechanistic understanding of deformation and rate-controlling mechanisms in nanocrystalline metals

As noted above, when the grain size of polycrystalline metals decreases from the micrometer scale down to the nanometer scale there are accompanying transitions in the mechanisms of inelastic deformation as well as significant changes in constitutive properties, including, inter alia, levels of strength, strain-rate sensitivity and strain hardening. There is direct experimental evidence for these transitions (see e.g. [1,81,127,188,189]), theoretical evidence *vis-à-vis* and MD simulations of nanocrystalline deformation [15,166], as well as suspicions that arise from what is known about the mechanisms of plastic deformation in crystalline metals. For example, in fcc metals with grain sizes in the micron and larger size range, plastic deformation occurs via the generation and motion of intragranular slip, i.e. dislocation motion. This process is evidently difficult at grain sizes well into the submicron range. This is readily understood by simply noting that the crystallographic shear stresses required to generate and move dislocation segments that exist within the well characterized networks which evolve during plastic flow are on the order of Gb/ℓ, where G is the shear modulus, b the magnitude of the Burgers vector and ℓ the segment length. However, if dislocations are to be confined to the intragranular space, which might be taken as the definition of a grain, then ℓ must be less than the grain diameter, d. In fact, simulations of the operation of Frank–Read sources would suggest $\ell < d/4 - d/3$ (see e.g. [190]). This would lead to the conclusion that $\tau/G \geqslant (3-4)(b/d)$. For pure Ni, since $G \approx 82$ GPa, then if $d \approx 1$ μm, $\tau \geqslant 82$ MPa, which is reasonable. If, however, $d \approx 30$ nm then $\tau \approx 3280$ MPa, which is too large by at least a factor of nearly 3! This alone is an indication that dislocation nucleation in nanoscale grains may have to be assisted by grain boundary sources.

Insight into the operative flow process, dislocation or otherwise, can be gained through an examination of the characteristic deformation kinetics parameters extracted from macroscopic mechanical tests. For thermally activated plastic flow, the shear deformation rate in fcc metals is expressed as

$$\dot{\gamma} = \dot{\gamma}_0 \exp\left(-\frac{\Delta G(\tau_e^*)}{kT}\right) = \dot{\gamma}_0 \exp\left(\frac{-\Delta F + \tau_e^* \Delta V^*}{kT}\right) \qquad (3)$$

where k is the Boltzmann constant and T is the temperature. $\dot{\gamma}_0$ is a pre-exponential constant or a characteristic strain rate at a given grain size d, ΔG is the Gibbs free energy of activation for the stress-assisted, thermally activated flow process, and ΔF and ΔV^* are the Helmholtz free energy (activation energy) for overcoming obstacles to dislocation motion and the activation volume, respectively. In overcoming obstacles, free energy may be stored temporarily (e.g. by increased dislocation length) or permanently (e.g. by the creation of jogs after intersection). Processes of the former kind can be thermally activated, while the latter processes cannot. Consequently, the macroscopic shear stress may be divided in an *athermal part*, connected to structure, and a *thermal part*. Decisive for the athermal stress is whether it is of long-range nature, in which case it cannot be overcome by thermal activation. Consequently, under the influence of an external applied stress an effective stress (i.e. the applied stress corrected for the structural part) is available to move a dislocation across a barrier. The principal short-range barrier, the Peierls–Nabarro stress, is important for ufc/mc bcc metals, whereas in ufc/mc fcc and hcp metals, forest dislocations are the primary short-range barriers at lower temperatures. ΔG is a decreasing function of the effective shear stress τ_e^*, as the activation barrier is lowered by the work done by the effective stress, $\tau_e^* \Delta V^*$. $\Delta V^* = -(\partial \Delta G/\partial \tau_e^*)_T$ and τ_e^* is the thermal component of the total stress, τ, i.e. τ_e^* accounts for the stress needed to overcome the short-range barrier responsible for the temperature and strain-rate dependence, aside from the athermal contribution, τ_μ.

We next examine implications of Coble creep as the rate-controlling deformation process. In this case, the strain rate would be proportional to the stress and corresponds to the following scenario: in Eq. (3) deformation occurs at a relatively low stress and a high homologous temperature, such that the exponential stress activation term is small and the exponential becomes approximately linear in stress [191]. However, this assumption is not valid for the nc metals deformed at low homologous temperatures and ordinary strain rates, where at room temperature the stress term is of the order of 0.4 eV [120], much larger than kT. Therefore, the exponential dependence in Eq. (3) remains. In Section 3 we have shown that for nc Cu and Ni $m < 0.06$, which is more than a factor of 10 smaller than the value expected for the grain boundary diffusion mediated diffusional creep (where m would be on the order of unity). For diffusional creep the expected activation volume ΔV^* is of the order of atomic volume, i.e. b^3. But the activation volume determined from the recent strain rate change tests for nc Ni [120,137,192] and nc Cu [53,100] is more like $10–20b^3$. Grain boundary sliding mechanisms likewise entail m (≈ 0.5) and ΔV^* ($\approx b^3$) values that are inconsistent with experimental findings. Therefore such GB mechanisms are unlikely to dominate in the tensile deformation of nc metals with the grain size range in the current experimental samples. This assertion is consistent with the observation noted in Section 3 that the H–P strengthening relationship apparently holds for these grain sizes. Note that this discussion is not meant to imply that the GB diffusion-related mechanisms are absent. In fact, they may be, and should be, contributing to the plastic strain. Our argument is that they are not yet playing the dominant role to account for the bulk deformation rate,

until perhaps much smaller grain sizes of the order of a few nanometers. It must also be recalled that in most of the materials tested to date there existed grain size distributions that entailed significant volume fractions of grains whose sizes were very much larger than would be expected to display dominant deformation mechanisms such as diffusional creep or grain boundary sliding. For this reason as well, it is expected that such mechanisms were not dominant.

As indicated above, the activation volume, measured from strain rate change tests provides a signature of the dislocation mechanism. For nc Ni, a stress relaxation test can also be used to deduce an apparent activation volume of $20b^3$ [120]. The physically effective or true activation volume has been obtained from repeated stress relaxation tests [120], yielding a ΔV^* value of $10b^3$. Activation volumes of similar magnitude have been measured in nc Ni [119,137] and nc Cu [53,77]. It should be realized that strain rate change tests and stress relaxation tests may provide somewhat different answers for the activation volume. In particular, a stress relaxation test better approaches the boundary conditions of Eq. (2), i.e. a constant obstacle structure, than a strain-rate change test.

Three likely scenarios have been discussed to explain the small activation volume, relative to the hundreds or even thousands of b^3 known for the forest-dislocation cutting mechanisms of conventional fcc metals [120]. The rate-limiting thermally activated mechanism can be the punching of a mobile dislocation through a dense bundle of (excess) grain boundary dislocations, such as the case of nc metals prepared using severe plastic deformation where large numbers of excess dislocations reside in the vicinity of the so-called non-equilibrium GBs. For other types of nc metals, the small activation volume is more likely associated with the critical size of a dislocation emitted from a GB (i.e. a defect-assisted dislocation nucleation mechanism [127]), or the local volume involved in the de-pinning of a propagating dislocation [128] that is pinned by (impurity decorated) grain boundaries, at an obstacle such as grain boundary ledges. These are unusual activated processes in the sense that they are insignificant for coarse-grained metals where intragrain dislocations abound and dominate plastic deformation. The dislocation–grain boundary interaction-mediated mechanisms become increasingly important with decreasing grain size, and dominant in nc metals. This is because in nc metals the extremely small grain sizes make it difficult for intragrain dislocation sources to operate and leave little room for cross slip, but offer a high density of nonequilibrium grain boundaries, grain boundary dislocation sources and pinning sites.

Recent model analyses [120,127,137] indicate that, due to the small volumes involved in the process of dislocations leaving/escaping from boundaries, the activation volume would be much smaller than those associated with the conventional mechanisms of forest dislocation intersection in the lattice; this in turn would be associated with a correspondingly elevated strain-rate sensitivity. For example, when one views the process as "either dislocation nucleation or de-pinning from the boundary during its propagation" [127,128], the process would entail an activation length that is a fraction of that of the edge of a grain. The difficulties associated with "dislocation escaping" from these boundaries would lead to a higher activation energy, as well as a stronger temperature dependence of the strength. In other words, the relatively loose and weak barriers in normal fcc lattices are now replaced by harder obstacles concentrated at the boundaries. We will examine the case of dislocation emission from grain boundary in more detail below.

4.2.1. Perfect and partial dislocation emission

Fig. 10a illustrates a process of emission of a dislocation from a grain boundary into the interior of a grain [6,127]. Note that the figure describes details associated with the emission of a partial dislocation, but it can also be used to explain the result of the emission of a perfect dislocation. As explained by Asaro et al. [6], as the segment is emitted into the grain it creates two trailing segments in the "side grain boundaries", and, in the case of a partial dislocation, a stacking fault within the grain. The energy (per unit length) of these segments is taken as $1/2Gb^2$ for the perfect dislocation and $1/6Gb^2$ for the partial dislocation. The explanation for the latter value lies simply in the fact that, for a Shockley partial dislocation in a fcc crystal, the magnitude of the Burgers vector is $b_{\text{partial}} = 1/\sqrt{3}b_{\text{perfect}}$. As evident, $b = b_{\text{perfect}}$ is the magnitude of the perfect Burgers vector. Now in the case of the emission of a perfect dislocation, the minimum required resolved shear stress is that required to perform the work of creating the two residual segments in the side boundaries, or $\tau bd\delta x = 2(1/2)Gb^2\delta x$. This leads to the remarkably simple result, $\tau/G = (b/d)$. The d^{-1} scaling of stress level derives simply from the fact that the area over which work can be performed by the applied shear stress itself scales with d for a given δx. It is, additionally, typical for such micromechanical models to forecast strength levels that scale as d^{-1} rather than as $d^{-1/2}$. Moreover, as noted in Refs. [6,127], this leads to forecasted shear stresses that are too high for grain sizes less than, 20–30 nm for typical fcc metals for which data exist.

For the case of the emission of a partial dislocation, there is a reduced requirement for work associated with the residual segments in the side boundaries (owing to their lesser energy per unit length), but now an additional requirement to create a stacking fault with an energy Γ per unit area. The analysis of Asaro et al. [6] is not repeated here, but the result for the emission criterion is:

$$\{(\tau_{ms}/G)b_s^{(1)}/|b| + (\tau_{mz}/G)b_z^{(1)}/|b|\} = \frac{(\alpha-1)}{\alpha}\widetilde{\Gamma} + \frac{1}{3}(b/d) \tag{4}$$

where $\alpha \equiv d/\delta_{\text{eq}}$ and $\widetilde{\Gamma} \equiv \Gamma/Gb$. Thus if we define

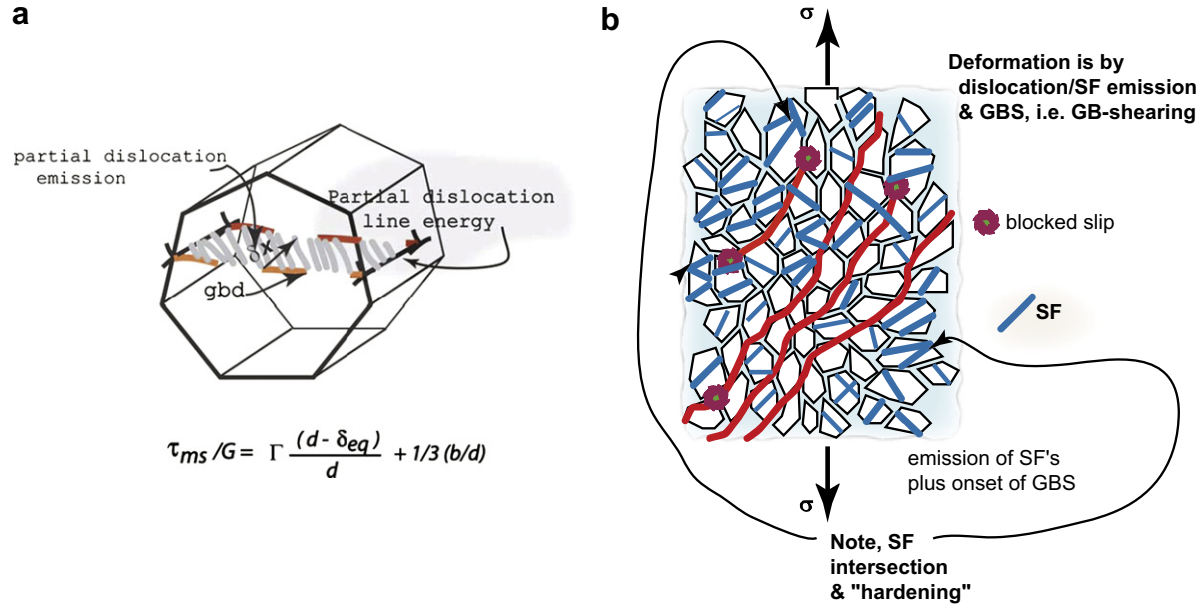

Fig. 10. (a) Emission of a perfect or partial dislocation from an existing dislocation at a grain boundary. As the leading partial dislocation enters the grain it produces partial segments along the side boundaries. (Figure taken from Ref. [127].) (b) A nanocrystalline aggregate model including dislocation and grain boundary sliding mechanisms of deformation. Note the zones of grain boundary shearing (or sliding) shown in red as well as intra-crystalline mechanisms as described in (a). (Figure taken from Ref. [92].)

$$\tau^{(\alpha)} \equiv \tau_{ms} b_s^{(1)}/|b| + \tau_{mz} b_z^{(1)}/|b| \tag{5}$$

we obtain

$$\tau^{(\alpha)}/G \approx \frac{1}{3}(b/d) + \frac{(\alpha-1)}{\alpha}\widetilde{\Gamma} \tag{6}$$

which is Asaro et al.'s Eq. (7) [6]. We also recall that δ_{eq} is defined as the equilibrium spacing of Shockley partials in the absence of applied stress and is given as

$$\delta_{eq} = \frac{1}{12\pi}(Gb^2)/\Gamma \tag{7}$$

The coordinate system of the dislocation's slip system is such that **m** is the unit normal to the slip plane, **s** is unit vector along the direction of the perfect Burgers vector, **b**, and **z** is the third of a right-handed unit triad and lies in the slip plane as well.

Some numerical predictions of critical resolved shear stress from Eqs. (6) and (7) for four FCC metals are listed in Table 1 [127].

Note that the combination of a relatively high stacking fault energy and modulus for Ni results in a predicted high strength level. On the other hand, the strength level for Pd, which has a high stacking fault energy, is similarly predicted to be relatively high, especially as compared with Cu, which has a shear modulus comparable to that of Pd but a lesser value for Γ. Ag is clearly predicted to show the lowest strength, which, although not surprising, should be appreciated as suggesting that nanostructuring will not lead to terribly high strengths. Note that, for Ag, $\delta_{eq} \approx 3.4$ nm, and thus when $d \sim 10$ nm little is to be gained from further reductions in grain size.

Fig. 10b puts the nanoscale mechanisms such as just described in the perspective of nanocrystalline aggregate response. Models for nc aggregates are discussed below in Section 4.2.3.

4.2.2. Nucleation of dislocations and twins at boundaries

The observed sensitivity to strain rate in nanocrystalline metals has been explained by Asaro and Suresh [127] in terms of the expected small activation volumes that are anticipated from models for the nucleation of defects such as partial or perfect dislocations at grain boundaries. Several types of mechanisms were considered including the emission of extended partial segments and dislocation loops from the sites of stress concentration. The possibility of sliding grain boundary facets was considered in detail, as illustrated in Fig. 10.

Table 1
Typical results of critical resolved shear stress generated from Eqs. (6) and (7)

d (nm)	50	30	20	10	δ_{eq}	$\Gamma/(Gb)$
Cu	211 MPa	248 MPa	291 MPa	421 MPa	1.6 nm	1/250
Ni	960 MPa	1027 MPa	1115 MPa	1381 MPa	0.5 nm	1/100
Ag	125 MPa	158 MPa	198 MPa	321 MPa	3.4 nm	1/447
Pd	719 MPa	763 MPa	820 MPa	988 MPa	0.54 nm	1/75

What was predicted, in particular, from models such as that shown in Fig. 11b was that the activation radii of nucleating loops, at applied shear stress levels approaching the athermal stress, are expected to be on the order of

$$r_c \approx (1 + 5\widehat{\Gamma}e + \frac{1}{2}[5\widehat{\Gamma}e]^2 + ...)er_0 \tag{8}$$

where $\widehat{\Gamma} = \Gamma/Gb_1$ is a reduced stacking fault energy. Some numerical examples follow. Since $1/500 \leqslant \widetilde{\Gamma} \leqslant 1/100$ for a wide range of fcc metals (see, e.g. Table 1), we find that $r_c \approx eb_1$ or $r_c \approx (e/\sqrt{3})b$. This suggests, while momentarily ignoring the effect of $\widehat{\Gamma}$, an activation volume on the order of $\Delta V^* \approx \frac{1}{6}\pi e^2 b^3 \approx \pi b^3$. To assess the effect of stacking fault energy, recall that $\widehat{\Gamma} = \sqrt{3}\widetilde{\Gamma}$. For Ni, for example, the result in Eq. (8) leads to the estimate $\Delta V^* \approx 5.3b^3$. At corresponding values of applied shear stress below that which exists at this state, the activation area will be larger, but nonetheless such small activation volumes are consistent with the high strain-rate sensitivity evident in the data. In particular, activation volumes of the order $5 - 10b^3$ are readily rationalized by the mechanisms we suggest here.

4.2.3. Aggregate models

Experimental techniques available for the full characterization of structure at the nanoscale have been primarily based on TEM and XRD, from which the average grain size and grain size distributions can be estimated, subject to statistical uncertainty that we specifically address here. For grain size distributions, the numbers of grains of various diameters in nanocrystalline materials can usually be well represented by a log-normal distribution function

$$P(D) = \frac{1}{(2\pi)^{1/2}D\sigma}\exp\left[-\frac{1}{2}\left(\frac{\ln(D/D_0)}{\sigma}\right)^2\right] \tag{9}$$

where the symbol D is used for the grain diameter and D_0 and σ are constant parameters describing the median and shape parameters (i.e. the standard deviation of $\ln D$) of the distribution respectively and $\int_0^\infty P(D)\,dD = 1$. The arithmetic mean size $\bar{D}$ can be calculated [193] as

$$\overline{D} = D_0 \exp\left(\frac{1}{2}\sigma^2\right) \tag{10}$$

It is important, however, to realize that within typical grain size distributions it is the members of the larger group of grain size that dominate the volume fraction and thus the overall response of the aggregate. The aggregate model of Zhu et al. [92,93] was, in fact, specifically developed to account for this. Their model is a physically based, finite strain, crystal plasticity theory and envisions that grain interiors can deform by the mechanisms of perfect or partial dislocation emission from grain boundaries or by grain boundary sliding. For example, as caused by the emission of partial dislocations, the law governing the slip rate in a nanocrystalline grain is phrased as

$$\dot{\gamma}^{(\alpha)} = \begin{cases} \dot{\gamma}_0\left\{\frac{\tau^{(\alpha)}/G - \tilde{\alpha}\widetilde{\Gamma}}{g^{(\alpha)}}\right\}^{1/m} & \text{if } \tau^{(\alpha)}/G - \tilde{\alpha}\widetilde{\Gamma} > 0 \\ 0 & \text{otherwise} \end{cases} \tag{11}$$

and a similar relation based on the Asaro et al. [6] model is applied, in parallel, to describe slip via perfect dislocation emission. Here $\tilde{\alpha} = (\alpha - 1)/\alpha$. Thus both perfect and partial dislocations are emitted simultaneously based on a consistent set of criteria.

For grain boundary sliding, the phenomenological rate law proposed by Conrad and Narayan [194], viz.

$$\dot{\gamma} = \frac{6bv_D}{d}\sinh(v\bar{\tau}/kT)\exp(-\Delta F/RT) \tag{12}$$

was used as an *effective plastic strain rate* within the framework of a J_2-flow theory of plasticity.

Simulations were carried out by Zhu et al. [92] for common fcc metals that at least limited data were available for. For example, simulations were performed for electrodeposited Ni for which the grain size distributions were documented [104]. For such materials, the average grain size was in the range 20–25 nm. Results are shown for predicted uniaxial tension at 20 °C in Fig. 12. Experimental results for Ni with an average grain size of 23 nm is superposed on the predicted curves calculated at the three strain rates indicated. The computed strain rate sensitivity is in agree-

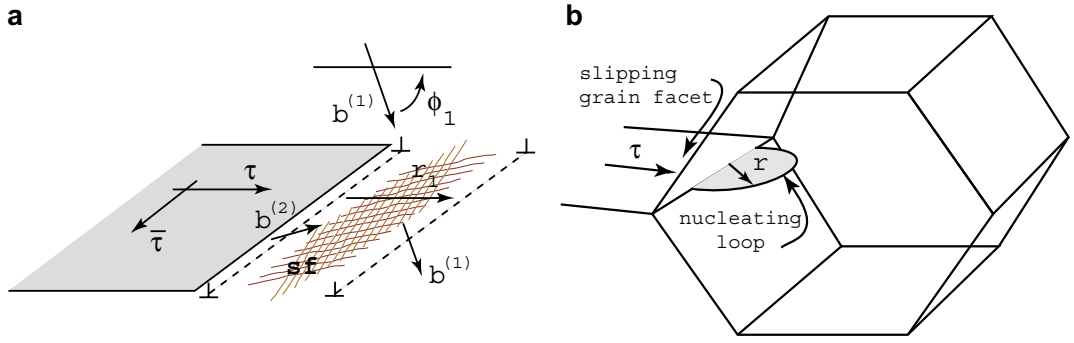

Fig. 11. (a) A model for partial dislocation emission from a grain boundary that acts in a crack-like manner. The crack is loaded via an in-plane Mode II applied stress, τ, and an anti-plane Mode III shear stress, $\bar{\tau}$. (b) Nucleation of a partial dislocation loop at the front of a freely slipping grain boundary facet. (Figure taken from Ref. [127].)

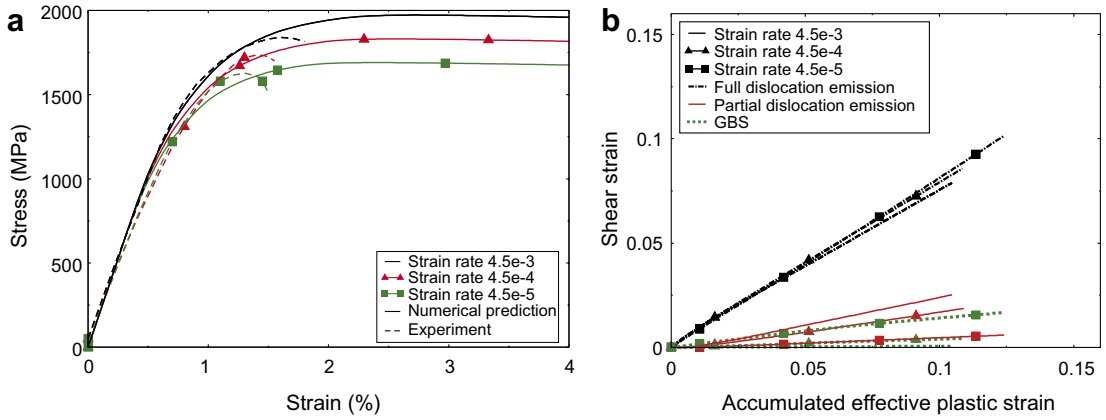

Fig. 12. Computed stress vs. strain response (left side figure) for nanocrystalline Ni with average grain size of 23 nm and variance of 60 as in Eq. (9). Contribution to the overall plastic strain arising from the three deformation mechanisms considered but for a simulated nanocrystal with a mean grain size of 10 nm and a variance of 50. All simulations are carried out at 20 °C. (Figure taken from Ref. [92].)

ment both with what was shown in Fig. 6b and with respect to the predictions of the Asaro and Suresh [127] models discussed briefly above. Fig. 12b shows the computed contribution of each of the three mechanisms to the overall deformation. It should be noted that, for what turns out to be a quite typical grain size distribution, contributions from either grain boundary sliding or partial dislocation emission are minimal. In fact, it would be judged to be improbable that experimental attempts to observe the appearance of defects, such as stacking faults or deformation twins, would be successful, or at any rate definitive, in such materials since the occurrence of such defects would be confined to only the smaller grains and thus present in a small volume fraction of material. It may well be that, due to the dominance of the larger grains in the overall deformation, the aggregate's strength scales closer to $d^{-1/2}$ rather than to the d^{-1} as characteristic of nanoscale models for dislocation emission.

A recent study on fcc nc metals by Wei et al. [195] proposed a rate-dependent amorphous plasticity GB model which accounts for cavitation and related failure phenomena in nc GBs, in conjunction with a crystal plasticity model that is used for the grain interiors. Their simulation results on nc Ni show a transition in deformation mechanism from grain-interior shearing to grain-boundary shearing, as the average grain size decreases from 50 to 10 nm. Low ductility of nc Ni was suggested to be the result of intergranular failure due to grain-boundary shearing and the resulting cavitation at triple-junctions and other high stress points in the microstructure.

Recent atomistic modeling, in addition to the MD modeling already mentioned, has begun to shed new light on processes such as grain boundary sliding [196–198]. To date, such modeling as in Sansoz and Molinari [196,197] has demonstrated that, for simple tilt boundaries, sliding is possible at shear stress levels achievable in nc fcc metals. Additional studies of this type, and those that account for finite temperatures, are needed to acquire a more complete understanding of the possible contributions of even local grain boundary sliding and its possible role in defect initiation at grain boundaries.

4.2.4. Stress-induced grain coarsening in Cu

As noted by Zhang et al. [84,85], the large excess energy associated with grain boundaries in nanocrystalline metals is expected to cause instability in their nc grain size distributions. Indeed, recent experiments [84,85] on indentation creep in high purity nanocrystalline Cu have shown that the hardness drops rapidly as the dwell time of the indenter in the sample increases. Grain growth was observed in these cases and undoubtedly was a primary cause of the decrease in hardness. By accounting for the effects of grain growth, Zhu et al. [93] were able to closely describe the decrease in hardness vs. indenter dwell time using their aggregate model presented above. Since the structure of the plastic zone was not then known, Zhu et al. [93] assumed that the volume fraction of the zone where grain growth occurred increased with the logarithm of time. This assumption was based on Zhang et al.'s observations of the decrease in hardness with time. The hardness was determined by the response of the zone of high stress or the plastic zone beneath the indenter. It is assumed that, with increasing dwell time, the grain growth zone spread and eventually occupied the entire plastic zone. Estimates indicated that the time it took for this was well over the 1800 s that was the largest time followed by Zhang et al. [84,85]. For simplicity, then, Zhu et al. [93] assumed that the volume fraction of the grain growth zone, with respect to the plastic zone, increased linearly from 0% to 100% in a time t_f. They assumed the properties of the material to be a simple average of those of the original distribution and those associated with the grown grain size distribution, i.e. if $\mathscr{R}$ is the volume fraction of the grain growth zone with respect to the plastic zone, then the properties were computed as $\mathscr{R} \times \mathscr{P}_{\text{grown}} + (1 - \mathscr{R}) \times \mathscr{P}_{\text{original}}$ where $\mathscr{P}_{\text{grown}}$ and $\mathscr{P}_{\text{original}}$ figuratively represent the constitutive properties of material with the respective coarsened and original grain size distributions. Hardness was estimated by first

simulating the ultimate strength in uniaxial tension and assuming the hardness to be equal to $3\sigma_{\text{ultimate}}$.

What was found, in fact, was that the process of grain growth and hardness decrease did not saturate, even after the longest dwell times applied by Zhang et al. [84,85].

Fig. 13 shows results for the predicted hardness decrease with time based on a wide range of assumed values for t_f such that $2\times10^3\ \text{s} \leqslant t_f \leqslant 10^8\ \text{s}$; also shown are Zhang et al.'s data [85]. What is clear is that as long as $t_f \geqslant 10^4$ s the agreement between prediction and experimental measurement is good. Thus, what is unknown, but of vital importance, is at what times the grain growth process would saturate and how far the hardness would decrease. A corollary to this would be the question: is there a critical grain size distribution (shifted to larger grain sizes) that would be stable? Thus, despite the consistency between simulations of Zhu et al. [93] and the observations of Zhang et al. [84,85], it is clear that far more remains to be understood about the critical process of stress-induced grain growth.

Other such models that have explicitly identified grain size distribution as being of primary importance are those of Morita et al. [199]. These have also described grain size distributions within the framework of log-normal distributions and revealed the importance of rigorously accounting for it. In particular, Morita et al. [199] note that in typical grain size distributions the smallest grains are likely to contribute little to the overall aggregate response, an observation reconfirmed by our analysis herein. The data of Ebrahimi et al. [200,201], especially as they are interpreted based on an assessment of non-deforming vs. deforming grains, also demonstrate the importance of size distribution even at fixed average grain size.

The phenomenon of grain growth in nc metals is of fundamental importance for a number of reasons, including (1) the significant effect the process has on diminishing the enhanced mechanical properties; and (2) the process being clearly related to the most basic underpinnings of deformation mechanisms in nc metals. The phenomenon occurs not just in metals with grain sizes less than, say, 20 nm, but in metals with grain sizes in the 50–60 nm size range as well (see e.g. [88]). No model yet exists for the process and the overall phenomenology is only beginning to be uncovered. Preliminary micromechanical models for nc grain migration have been proposed (e.g. [202]), and these, along with those likely to follow, will be helpful in suggesting the way to understanding the operative mechanisms. For simple tilt boundaries, for example, Gutkin and Ovid'ko [202] developed a micromechanics based criteria for a critical shear stress, τ_{cr}, for boundary motion, viz.

$$\frac{\tau_{cr}}{G} \approx \frac{\omega}{2\pi(1-\nu)}\frac{b}{d}\ln\left(\frac{d}{b}\right), \quad b < d \tag{13}$$

where ω is the tilt angle. The result is interesting in that, for tilt angles in the range $5^\circ \leqslant \omega \leqslant 30^\circ$ and for grain sizes in the range $10\ \text{nm} \leqslant d \leqslant 30\ \text{nm}$, τ_{cr} is found to be in the range 20–300 MPa, well in the prevailing range of stress levels for many fcc metals with grain sizes in that range. A full understanding of grain boundary mobility and grain growth, however, will await more detailed experiment and detailed atomistic modeling. Atomistic modeling will have to include a nonisothermal response and gradually approach realistic stress and strain rate levels.

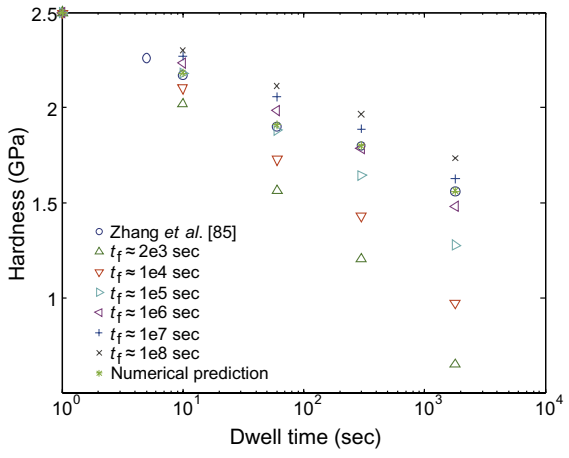

Fig. 13. Simulated hardness vs. time [93], compared with the measurements of Zhang et al. [85]. The simulations were performed using a wide range for t_f, i.e. $2\times10^3\ \text{s} \leqslant t_f \leqslant 10^8$ s. (Figure taken from Ref. [93].)

4.2.5. Deformation in presence of nanoscale growth twins

A comprehensive computational analysis of the deformation of ultrafine crystalline pure copper with nanoscale growth twins was recently carried out [78]. This physically motivated crystal plasticity model benefited from earlier experimental studies, in particular post-deformation TEM investigations of dislocation structures in the Cu containing high densities of nanoscale growth twins [25,76,78]. The post-tensile TEM microstructure observations suggest that the interaction of dislocations with TBs plays a crucial role in the plastic deformation for the nt-Cu. Abundant dislocation debris is seen in the vicinity of TBs/GBs in nt-Cu-fine, as shown in Ref. [76]. Compared with the relatively defect-free microstructure of as-deposited nt-Cu-fine, the typical structure of the deformed specimen is populated with a high density of dislocations [25,76,78]. TBs with copious dislocations and debris are not as clear, sharp and straight as the original coherent TBs in the as-deposited condition, whereas stepped (the arrows in Fig. 14a) or even curved TBs (see the white rectangle A in Fig. 14a) are frequently seen. It is clearly observed that in Fig. 14a, within a few nanometers of the TBs, the crystal lattice is often elastically strained due to the high density of the dislocation debris accumulated along the TBs during deformation. An HRTEM observation (Fig. 14b) shows that a high density of dislocation debris, identified as Shockley partial dislocations, is deposited along TBs in nt-Cu-fine [25,76,78].

TEM observations suggest that most of the plastic strain is carried by the dislocations piling up along the TBs, which results in shear strain accumulation at the TBs. TBs are likely to take on much more strain than the internal volume

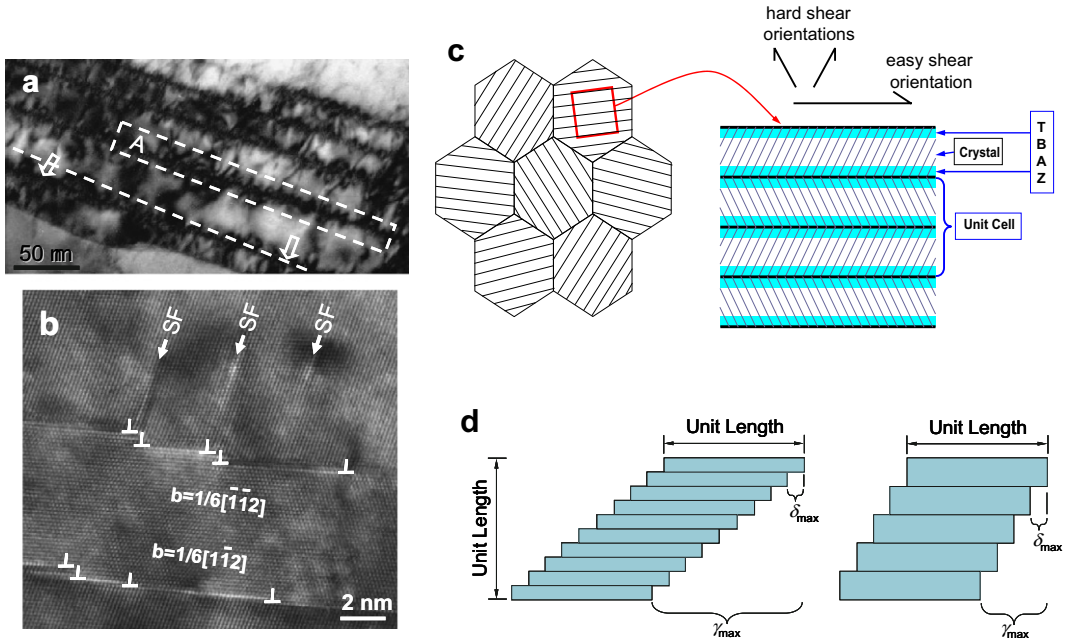

Fig. 14. (a) TEM observation of an nt-Cu-fine sample after tensile test showing dislocation pile ups along TBs and curved TBs; a region within a few nanometers of a TB is often heavily influenced by the dislocations along the TBs. (b) HRTEM of an nt-Cu-fine sample, showing partial dislocation disassociation, dislocation pile up and TB bending. (c) Schematic drawing of the proposed twin boundary affected zone (TBAZ) model, where TBAZ refers to the region adjoining the twin boundaries where the crystalline lattice is elastically strained. (d) A simple strain-based damage/failure criterion. The model assumes that each TB can accommodate δ_{max} amount of slip deformation per unit length, i.e. $\gamma_{max} = n\delta_{max}$, where n is the number of TBs per unit length (i.e. twin density). It is clear that local ductility is directly proportional to the twin density with this assumption. (Figure taken from Ref. [78].)

residing beyond a few nanometers away from the TBs. The steps observed in the deformed TBs [25,76,78] indicate that dislocations can also propagate across initially coherent TBs, as discussed by Mahajan and Chin [203] and Christian and Mahajan [204] and indicated via MD simulations by Jin et al. [186]. Screw dislocations interacting with twin boundaries and closely related grain-boundaries were analyzed earlier by Pestman et al. [187]. It was found that transmission occurred at a minimum of three times the friction stress, indicating that the TB is an obstacle to dislocation motion. It was also found that there exists an attractive force between the TB and a (partial) dislocation core. This can be explained by considering that the dislocation lowers the energy of its core in various ways by merging in the TB. In the case of TB absorption of the partial dislocation core in the boundary plane, it was observed in the atomistic calculations as the minimum energy configuration [187]. More recently, Dewald and Curtin [205] carried out a coupled atomistic/discrete-dislocation multiscale methodology to study screw dislocations interacting with Σ3, Σ11 and Σ9 symmetric tilt boundaries in Al. The low-energy Σ3 boundary absorbs lattice dislocations and generate extrinsic grain boundary dislocations (GBDs). As multiple screw dislocations impinge on the GB, GBDs pile up along the GB and provide a back stress that requires increasing applied load to push the lattice dislocations into the GB. Interestingly, dislocation transmission is hardly observed, even with large GBD pile-ups near the dislocation/GB intersection. The interactions of dissociated lattice dislocations with a near Σ3 grain boundary in copper was investigated by TEM using the weak-beam technique [206]. These observations support the aforementioned theoretical findings, namely that Shockley partials are required to recombine when entering the GB to form an absorbed perfect lattice dislocation. Complex reactions between the resulting displacement shift complete dislocations after absorption yield further stress relaxation.

Motivated by the TEM and MD observations, a twin boundary affected zone (TBAZ) model was proposed [78], where each TB is considered as a special GB with a high aspect ratio in terms of the grain shape and mirrored slip geometries between adjacent twin lamellae. The so-called TBAZ refers to the region adjoining the twin boundaries where the crystalline lattice is elastically strained although no obvious lattice defects may be observed prior to plastic deformation. The following assumptions were made [78] with respect to the TBAZ model (see Fig. 14c): (1) a TBAZ within the nanoscale twin lamellae spans on the order of about 7–10 lattice parameters away from the TB, which is on the same order as a grain boundary affected zone (GBAZ) (see [3,103] for detailed discussions regarding GBAZ); (2) the TBAZ is considered plastically softer than the predominantly elastic crystal interior region between TBAZs at the nanoscale; (3) there is a significant plastic anisotropy between the shear deformation parallel to the TBs and the shear deformation transverse to the TBs; and (4) the TBAZ deforms with a relatively larger rate sensitivity than the crystal interior region, due to locally concentrated dislocation activities with a small activation volume.

Fig. 14d schematically shows a simple strain-based failure/damage model for nt-Cu samples, where the local ductility is directly proportional to the twin density. Fig. 15 shows the simulation results of the model. This model correctly predicts the experimentally observed trends (see Fig. 2a) of the effects of twin density on flow strength, rate sensitivity of plastic flow and ductility, in addition to matching many of the quantitative details of plastic deformation reasonably well [78].

The computational simulations provide critical mechanistic insights into why the metal with nanoscale twins can provide the same level of yield strength, hardness and strain-rate sensitivity as a nanostructured counterpart without twins (but of grain size comparable to the twin spacing of the nano-twinned Cu). The analysis also offers some useful understanding of why the nano-twinned Cu with high strength does not lead to diminished ductility with structural refinement involving twins. A very recent atomistic model on nt-Cu by Zhu et al. [207] showed that the TB-mediated slip transfer reactions are the rate-controlling mechanisms of plastic deformation. The predicted activation volume and rate-sensitivity exponent were found to be comparable to the experimentally measured values [207]. The atomistic reaction pathway simulations were obtained at realistic strain rates using an improved version of the climbing image nudged elastic band method originally proposed in Ref. [208]. The simulation results [207] suggested that the relatively high ductility of nt-Cu is closely related to the hardening of twin boundaries as they gradually lose coherency during plastic deformation.

4.2.6. Future opportunities

The central message of Section 4 is that, with recent advances in experimental studies (especially HRTEM investigations on microstructure) and MD simulations, the deformation mechanisms and their relative importance during plastic deformation of nc/ns materials are being identified. For nc materials with an average and entire range of grain size between 10 and 100 nm, the deformation mechanism relative to intra-grain Frank–Read sources and forest dislocation hardening, which is prevalent in conventional mc materials, no longer operates effectively. Partial (or perfect) dislocation mediated processes interacting with GBs become dominant, while only a small amount of plasticity may be accumulated through grain boundary sliding/shearing processes. Based on these new advances, mechanistic analytical models and quantitative and mechanisms based constitutive continuum computations that can realistically capture experimentally measured and grain-size-dependent stress–strain behavior, strain-rate sensitivity and even ductility limit began to emerge.

There are still many outstanding questions remain to be investigated. First, it is important to verify that the in situ or ex situ TEM observations are truly bulk processes in nc materials. Second, MD simulations to understand detailed deformation processes are needed for ns materials with nanoscale twins. Third, detailed mechanics-based fracture and fatigue models for nc materials similar to those widely used in mc materials and engineering practices are still essentially undeveloped. Fourth, it remains a challenge to develop mechanisms-based models that can capture detailed grain boundary characteristics (different GB angles, pre-existing defects, interstitial foreign atoms, etc.). Fifth, a quantitative constitutive description of the deformation twinning in nc materials is still missing. Sixth, more definitive and rigorous models for the dynamic grain growth during deformation are needed. Seventh, constitutive models that can quantitatively guide the experiments for mechanical property optimization should be developed. In this overview the role of triple junctions in nc materials and the collective behavior of grains was not highlighted. For a description of effects of triple junctions, reference is made to a recent review [209].

Clearly, future research opportunities abound albeit are quite challenging.

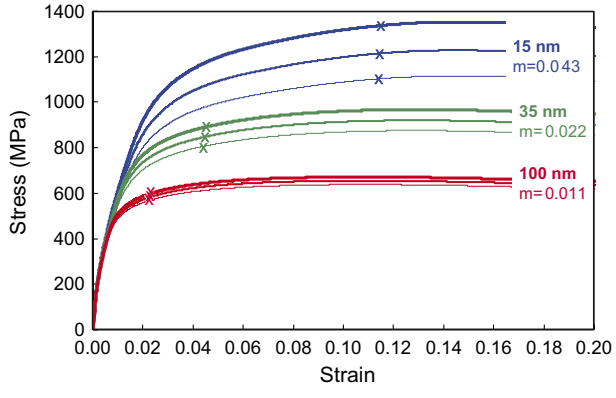

Fig. 15. Crystal plasticity simulation results of stress–strain curves and strain-rate sensitivity, m. (Figure taken from Ref. [78].) The top, middle and bottom three-curve sets show results of 15 nm (nt-Cu-fine), 35 nm (nt-Cu-medium) and 100 nm (nt-Cu-coarse) nt-Cu specimens, respectively. The strain rates simulated are $6\times10^{-3}\ s^{-1}$, $6\times10^{-2}\ s^{-1}$ and $6\times10^{-1}\ s^{-1}$, respectively. The symbol "X" denotes the predicted damage/failure initiation point.

5. Summary and concluding remarks

We have outlined recent progresses made in a number of areas related to the mechanical properties of nc/ns materials, including strength, ductility, strain rate and temperature dependence, fatigue and tribological properties, and related efforts to quantitatively and mechanistically understand the underlying deformation mechanisms. Our focus has been on pure fcc nc metals, where the most systematic experimental data are available. We have highlighted some of the most recent experimental results and mechanisms-based quantitative analyses without, due to space limitations, giving a detailed account of all developments in this field. The highlighted examples include the recent experimental studies in obtaining both high strength and considerable ductility, the compromise between enhanced fatigue limit and reduced crack growth

resistance, the stress-assisted dynamic grain growth during deformation, and the relation between rate sensitivity and possible deformation mechanisms. Recent developments in obtaining a quantitative and mechanics-based understanding of nc/ns mechanical properties are discussed, with particular emphasis on the mechanistic models of partial/perfect-dislocation or deformation-twin mediated processes interacting with grain boundaries, constitutive modeling and simulations of grain size distribution and dynamic grain growth in nc materials, and physically motivated crystal plasticity modeling of pure Cu with nanoscale twins.

These recent progresses have, on the one hand, pointed to promising routes to optimize mechanical properties, and on the other, presented new challenges to the understanding of intrinsic nc behaviors that require further investigations. A number of outstanding issues and possible future research directions are listed and proposed in respective sections. All these opportunities and efforts have brought, and will continue to bring, a more quantitative and mechanisms-based understanding of the mechanical behavior of nc materials.

Acknowledgments

M.D. acknowledges the financial support of the Defense University Research Initiative on Nano Technology (DURINT), which is funded at MIT by ONR under Grant N00014-01-1-0808. L.L. acknowledges National Science Foundation of China under Grant Nos. 50021101 and 50571096, and MOST of China (Grant No. 2005CB623604). R.J.A. is thankful to the National Science Foundation for support under the NIRT initiative. J.DeH. acknowledges support from the Netherlands Institute for Metals Research and the National Science Foundation of the Netherlands (The Hague, Physics Division, Fundamental Research on Matter-FOM). E.M. is supported at JHU by US NSF-DMR-0355395.

References

[1] Gleiter H. Prog Mater Sci 1989;33:223–315.
[2] Rack HJ, Cohen M. Mat Sci Eng 1970;6(5):320–6.
[3] Kumar KS, Van Swygenhoven H, Suresh S. Acta Mater 2003;51(19):5743–74.
[4] Koch CC. Scripta Mater 2003;49(7):657–62.
[5] Van Swygenhoven H. Science 2002;296(5565):66–7.
[6] Asaro RJ, Krysl P, Kad B. Philos Mag Lett 2003;83(12):733–43.
[7] Valiev RZ, Islamgaliev RK, Alexandrov IV. Prog Mater Sci 2000;45(2):103–89.
[8] Zhu YT, Langdon TG. JOM 2004;56(10):58–63.
[9] Meyers MA, Mishra A, Benson DJ. Prog Mater Sci 2006;51(4):427–556.
[10] Ma E. JOM 2006;58(4):49–53.
[11] Gleiter H. Adv Mater 1992;4(7–8):474–81.
[12] Gleiter H. Acta Mater 2000;48(1):1–29.
[13] Weertman JR. Mechanical behavior of nanocrystalline metals. In: Koch CC, editor. Nanostructured materials: processing, properties and potential applications. Norwich (NY): Willia. Andrew Publishing; 2002. p. 393–417.
[14] Cheng S, Spencer JA, Milligan WW. Acta Mater 2003;51(15):4505–18.
[15] Wolf D, Yamakov V, Phillpot SR, Mukherjee A, Gleiter H. Acta Mater 2005;53(1):1–40.
[16] Nieman GW, Weertman JR, Siegel RW. J Mater Res 1991;6(5):1012–27.
[17] Haas V, Gleiter H, Birringer R. Scripta Metall 1993;28(6):721–4.
[18] Sanders PG, Fougere GE, Thompson LJ, Eastman JA, Weertman JR. Nanostruct Mater 1997;8(3):243–52.
[19] Suryanarayana C. Prog Mater Sci 2001;46(1–2):1–184.
[20] Fecht HJ, Hellstern E, Fu Z, Johnson WL. Metall Trans A 1990;21(9):2333–7.
[21] Witkin DB, Lavernia EJ. Prog Mater Sci 2006;51(1):1–60.
[22] Erb U. Nanostruct Mater 1995;6(5–8):533–8.
[23] Elsherik AM, Erb U. J Mater Sci 1995;30(22):5743–9.
[24] Lu L, Sui ML, Lu K. Science 2000;287(5457):1463–6.
[25] Lu L, Shen YF, Chen XH, Qian LH, Lu K. Science 2004;304(5669):422–6.
[26] Lu K. Mater Sci Eng R-Rep 1996;16(4):161–221.
[27] Haberland H, Karrais M, Mall M, Thurner Y. J Vac Sci Technol A 1992;10(5):3266–71.
[28] De Hosson JTM, Palasantzas G, Vystavel T, Koch SA. JOM 2004;56(1):40–5.
[29] Koch SA, Palasantzas G, Vystavel T, De Hosson JTM, Binns C, Louch S. Phys Rev B 2005;71(8):085410.
[30] Vystavel T, Palasantzas G, Koch SA, De Hosson JTM. Appl Phys Lett 2003;82(2):197–9.
[31] Vystavel T, Koch SA, Palasantzas G, De Hosson JTM. J Mater Res 2005;20(7):1785–91.
[32] Cavaleiro A, De Hosson JTM. Nanostructured coatings. New York: Springer-Verlag; 2006.
[33] Birringer R, Gleiter H. Encyclopedia of material science and engineering: supplement 1. Oxford: Pergamon Press; 1988. p. 339.
[34] Gleiter H. Phys Blaetter 1991;47(8):753–9.
[35] Koch CC, Cho YS. Nanostruct Mater 1992;1(3):207–12.
[36] de la Rive A. Compt Rend 1837;4:835.
[37] Rösing B. Zeitschrift für Elektrochemie, Deutschen Electrochemischen Gesellschaft 1896;2(25):550–2.
[38] Natter H, Schmelzer M, Hempelmann R. J Mater Res 1998;13(5):1186–97.
[39] Choo RTC, Toguri JM, Elsherik AM, Erb U. J Appl Electrochem 1995;25(4):384–403.
[40] Cziraki A, Fogarassy B, Gerocs I, Tothkadar E, Bakonyi I. J Mater Sci 1994;29(18):4771–7.
[41] Bakonyi I, TothKadar E, Pogany L, Cziraki A, Gerocs I, VargaJosepovits K, et al. Surf Coat Technol 1996;78(1–3):124–36.
[42] Detor AJ, Schuh CA. Acta Mater 2007;55(1):371–9.
[43] Choi IS, Dao M, Suresh S. J Mech Phys Solids [submitted for publication].
[44] Choi IS, Detor AJ, Schwaiger R, Dao M, Schuh CA, Suresh S. J Mech Phys Solids [submitted for publication].
[45] Lu K, Lu J. J Mater Sci Tech 1999;15(3):193–7.
[46] Lu K, Lu J. Mater Sci Eng A 2004;375–377:38–45.
[47] Tao NR, Wang ZB, Tong WP, Sui ML, Lu J, Lu K. Acta Mater 2002;50(18):4603–16.
[48] Wang K, Tao NR, Liu G, Lu J, Lu K. Acta Mater 2006;54(19):5281–91.
[49] Erb U, Palumbo G, Szpunar B, Aust KT. Nanostruct Mater 1997;9:261–70.
[50] Su JQ, Nelson TW, Sterling CJ. J Mater Res 2003;18(8):1757–60.
[51] Hall EO. Proc Phys Soc London, Sect B 1951;64:747–53.
[52] Petch NJ. J Iron Steel Inst, London 1953;174:25.
[53] Chen J, Lu L, Lu K. Scripta Mater 2006;54(11):1913–8.
[54] Sanders PG, Eastman JA, Weertman JR. Acta Mater 1997;45(10):4019–25.
[55] Youssef KM, Scattergood RO, Murty KL, Koch CC. Appl Phys Lett 2004;85(6):929–31.

[56] Gray GT, Lowe TC, Cady CM, Valiev RZ, Aleksandrov IV. Nanostruct Mater 1997;9(1–8):477–80.
[57] Haouaoui M, Karaman I, Maier HJ, Hartwig KT. Metall Trans A 2004;35(9):2935–49.
[58] Meyers MA, Chawla KK. Mechanical behavior of materials. Upper Saddle River (NJ): Prentice-Hall; 1999.
[59] Ma E. Scripta Mater 2003;49(7):663–8.
[60] Ebrahimi F, Zhai Q, Kong D. Scripta Mater 1998;39(3):315–21.
[61] Hayashi K, Etoh H. Mater Trans JIM 1989;30(11):925–31.
[62] Valiev RZ, Alexandrov IV, Zhu YT, Lowe TC. J Mater Res 2002;17(1):5–8.
[63] Knapp JA, Follstaedt DM. J Mater Res 2004;19(1):218–27.
[64] Schuh CA, Nieh TG, Iwasaki H. Acta Mater 2003;51(2):431–43.
[65] Suryanarayanan Iyer R, Frey CA, Sastry SM, Waller BE, Buhro WE. Mater Sci Eng A 1999;264:210–4.
[66] Jiang HG, Zhu YT, Butt DP, Alexandrov IV, Lowe TC. Mater Sci Eng A 2000;290(1–2):128–38.
[67] Agnew SR, Elliott BR, Youngdahl CJ, Hemker KJ, Weertman JR. Mater Sci Eng A 2000;285(1–2):391–6.
[68] Valiev RZ, Kozlov EV, Ivanov YF, Lian J, Nazarov AA, Baudelet B. Acta Metall 1994;42(7):2467–75.
[69] Van Swygenhoven H, Caro A, Farkas D. Scripta Mater 2001;44(8–9):1513–6.
[70] Schiøtz J, Jacobsen KW. Science 2003;301(5638):1357–9.
[71] Argon AS, Yip S. Philos Mag Lett 2006;86(11):713–20.
[72] Conrad H. Mater Sci Eng A 2003;341(1–2):216–28.
[73] Schiøtz J, Di Tolla FD, Jacobsen KW. Nature 1998;391(6667):561–3.
[74] Van Vliet KJ, Tsikata S, Suresh S. Appl Phys Lett 2003;83(7):1441–3.
[75] Schuh CA, Nieh TG, Yamasaki T. Scripta Mater 2002;46(10):735–40.
[76] Lu L, Schwaiger R, Shan ZW, Dao M, Lu K, Suresh S. Acta Mater 2005;53(7):2169–79.
[77] Shen YF, Lu L, Lu QH, Jin ZH, Lu K. Scripta Mater 2005;52(10):989–94.
[78] Dao M, Lu L, Shen YF, Suresh S. Acta Mater 2006;54(20):5421–32.
[79] Shen YF, Lu L, Dao M, Suresh S. Scripta Mater 2006;55(4):319–22.
[80] Dahlgren SD, Nicholson WL, Merz MD, Bollmann W, Devlin JF, Wang DR. Thin Solid Films 1977;40(January):345–53.
[81] Gertsman VY, Hoffmann H, Gleiter H, Birringer R. Acta Metall 1994;42(10):3539–44.
[82] Valiev RZ. Mater Sci Eng A 1997;234:59–66.
[83] Wang YM, Chen MW, Zhou FH, Ma E. Nature 2002;419(6910):912–5.
[84] Zhang K, Weertman JR, Eastman JA. Appl Phys Lett 2004;85(22):5197–9.
[85] Zhang K, Weertman JR, Eastman JA. Appl Phys Lett 2005;87(6):061921.
[86] Jin M, Minor AM, Stach EA, Morris JW. Acta Mater 2004;52(18):5381–7.
[87] Soer WA, De Hosson JTM, Minor AM, Morris JW, Stach EA. Acta Mater 2004;52(20):5783–90.
[88] Liao XZ, Kilmametov AR, Valiev RZ, Gao HS, Li XD, Mukherjee AK, et al. Appl Phys Lett 2006;88(2):021909.
[89] Fan GJ, Wang YD, Fu LF, Choo H, Liaw PK, Ren Y, et al. Appl Phys Lett 2006;88(17):171914.
[90] Gianola DS, Van Petegem S, Legros M, Brandstetter S, Van Swygenhoven H, Hemker KJ. Acta Mater 2006;54(8):2253–63.
[91] Fan GJ, Fu LF, Qiao DC, Choo H, Liaw PK, Browning ND. Scripta Mater 2006;54(12):2137–41.
[92] Zhu B, Asaro RJ, Krysl P, Bailey R. Acta Mater 2005;53(18):4825–38.
[93] Zhu B, Asaro RJ, Krysl P, Zhang K, Weertman JR. Acta Mater 2006;54(12):3307–20.
[94] Koch CC, Morris DG, Lu K, Inoue A. MRS Bull 1999;24(2):54–8.
[95] Wang YM, Wang K, Pan D, Lu K, Hemker KJ, Ma E. Scripta Mater 2003;48(12):1581–6.
[96] He L, Ma E. Nanostruct Mater 1996;7(3):327–39.
[97] Legros M, Elliott BR, Rittner MN, Weertman JR, Hemker KJ. Philos Mag A 2000;80(4):1017–26.
[98] Wu XJ, Du LG, Zhang HF, Liu JF, Zhou YS, Li ZQ, et al. Nanostruct Mater 1999;12(1–4):221–4.
[99] Cheng S, Ma E, Wang YM, Kecskes LJ, Youssef KM, Koch CC, et al. Acta Mater 2005;53(5):1521–33.
[100] Wang YM, Ma E. Appl Phys Lett 2003;83(15):3165–7.
[101] Conrad H, Yang D. Acta Mater 2002;50(11):2851–66.
[102] Youssef KM, Scattergood RO, Murty KL, Horton JA, Koch CC. Appl Phys Lett 2005;87(9):091904.
[103] Schwaiger R, Moser B, Dao M, Chollacoop N, Suresh S. Acta Mater 2003;51(17):5159–72.
[104] Dalla Torre F, Van Swygenhoven H, Victoria M. Acta Mater 2002;50:3957–70.
[105] Karimpoor AA, Erb U, Aust KT, Palumbo G. Scripta Mater 2003;49(7):651–6.
[106] Zhang X, Wang H, Scattergood RO, Narayan J, Koch CC, Sergueeva AV, et al. Appl Phys Lett 2002;81(5):823–5.
[107] Yin WM, Whang SH, Mirshams R, Xiao CH. Mater Sci Eng A 2001;301:18–22.
[108] Kumar KS, Suresh S, Chisholm MF, Horton JA, Wang P. Acta Mater 2003;51(2):387–405.
[109] Hasnaoui A, Van Swygenhoven H, Derlet PM. Science 2003;300(5625):1550–2.
[110] Rice JR. Localization of plastic deformation. In: Koiter WT, editor. Proceedings of the 14th international congress of theoretical and applied mechanics. Amsterdam: North-Holland; 1976. p. 202–20.
[111] Li HQ, Ebrahimi F. Appl Phys Lett 2004;84(21):4307–9.
[112] Erb U. Presented at The 7th international conference on nanostructured materials (NANO' 2004), Wiesbaden, Germany; 2004.
[113] Zhang X, Wang H, Scattergood RO, Narayan J, Koch CC, Sergueeva AV, et al. Acta Mater 2002;50(19):4823–30.
[114] Wang YM, Ma E. Acta Mater 2004;52(6):1699–709.
[115] Lee Z, Witkin DB, Radmilovic V, Lavernia EJ, Nutt SR. Mater Sci Eng A 2005;410:462–7.
[116] Zhilyaev AP, Nurislamova GV, Kim BK, Baro MD, Szpunar JA, Langdon TG. Acta Mater 2003;51(3):753–65.
[117] Ma E, Wang YM, Lu QH, Sui ML, Lu L, Lu K. Appl Phys Lett 2004;85(21):4932–4.
[118] Wei Q, Kecskes L, Jiao T, Hartwig KT, Ramesh KT, Ma E. Acta Mater 2004;52(7):1859–69.
[119] Dalla Torre F, Spatig P, Schaublin R, Victoria M. Acta Mater 2005;53(8):2337–49.
[120] Wang YM, Hamza AV, Ma E. Acta Mater 2006;54(10):2715–26.
[121] Wei Q, Cheng S, Ramesh KT, Ma E. Mater Sci Eng A 2004;381(1–2):71–9.
[122] Lu L, Li SX, Lu K. Scripta Mater 2001;45(10):1163–9.
[123] Elmustafa AA, Tambwe MF, Stone DS. MRS Symp Proc 2003;70:Y8.14.1.
[124] Carreker Jr RP, Hibbard Jr WR. Acta Metall 1953;1(6):654–63.
[125] Zehetbauer M, Seumer V. Acta Metall 1993;41(2):577–88.
[126] Bochniak W. Acta Metall 1995;43(1):225–33.
[127] Asaro RJ, Suresh S. Acta Mater 2005;53(12):3369–82.
[128] Van Swygenhoven H, Derlet PM, Froseth AG. Acta Mater 2006;54(7):1975–83.
[129] Conrad H. J Metals 1964;16:582–8.
[130] Malis T, Tangri K. Acta Metall 1979;27(1):25–32.
[131] Taylor G. Prog Mater Sci 1992;36:29–61.
[132] Cahn JW, Nabarro FRN. Philos Mag A 2001;81(5):1409–26.
[133] Luthy H, White RA, Sherby OD. Mater Sci Eng A 1979;39(2):211–6.
[134] Coble RL. J Appl Phys 1963;34(6):1679–82.
[135] Champion Y, Langlois C, Guérin-Mailly S, Langlois P, Bonnentien J-L, Hÿtch MJ. Science 2003;300(5617):310–1.
[136] Wang YM, Ma E. Appl Phys Lett 2004;85(14):2750–2.
[137] Van Petegem S, Brandstetter S, Van Swygenhoven H, Martin JL. Appl Phys Lett 2006;89(7):073102.

[138] Suresh S. Fatigue of materials. Cambridge: Cambridge University Press; 1998.
[139] Agnew SR, Vinogradov AY, Hashimoto S, Weertman JR. J Electron Mater 1999;28(9):1038–44.
[140] Mughrabi H, Hoeppel HW. MRS Symp Proc 2001;634:B2.1.1–B2.1.12.
[141] Hanlon T, Kwon YN, Suresh S. Scripta Mater 2003;49(7):675–80.
[142] Hanlon T, Tabachnikova ED, Suresh S. Int J Fatigue 2005;27(10–12):1147–58.
[143] Suresh S. Metall Trans A 1985;16(2):249–60.
[144] Witney AB, Sanders PG, Weertman JR, Eastman JA. Scripta Metall 1995;33(12):2025–30.
[145] Villegas JC, Shaw LL, Dai K, Yuan W, Tian J, Liaw PK, et al. Philos Mag Lett 2005;85(8):427–37.
[146] Roland T, Retraint D, Lu K, Lu J. Scripta Mater 2006;54(11):1949–54.
[147] Farkas D, Willemann M, Hyde B. Phys Rev Lett 2005;94(16):165502.
[148] Han Z, Lu L, Lu K. Tribol Lett 2006;21(1):47–52.
[149] Bellemare S, Dao M, Suresh S. Int J Solids Struct 2007;44(6):1970–89.
[150] Leyland A, Matthews A. Wear 2000;246(1–2):1–11.
[151] Veprek S. J Vac Sci Technol A 1999;17(5):2401–20.
[152] Galvan D, Pei YT, De Hosson JTM. Acta Mater 2005;53(14):3925–34.
[153] Karch J, Birringer R, Gleiter H. Nature 1987;330(6148):556–8.
[154] Sherby OD, Wadsworth J. Prog Mater Sci 1989;33(3):169–221.
[155] Nieh TG, Wadsworth J, Wakai F. Int Mater Rev 1991;36(4):146–61.
[156] Voevodin AA, Zabinski JS. Thin Solid Films 2000;370(1–2):223–31.
[157] Tjong SC, Chen H. Mater Sci Eng R-Rep 2004;45(1–2):1–88.
[158] Pei YT, Galvan D, De Hosson JTM. Acta Mater 2005;53(17):4505–21.
[159] Meng WJ, Gillispie BA. J Appl Phys 1998;84(8):4314–21.
[160] Meng WJ, Tittsworth RC, Rehn LE. Thin Solid Films 2000;377:222–32.
[161] Patscheider J, Zehnder T, Diserens M. Surf Coat Technol 2001;146:201–8.
[162] Baker MA, Kench PJ, Tsotsos C, Gibson PN, Leyland A, Matthews A. J Vac Sci Technol A 2005;23(3):423–33.
[163] Johnson WL. MRS Bull 1999;24(10):42–56.
[164] Leyland A, Matthews A. Surf Coat Technol 2004;177:317–24.
[165] Jia D, Ramesh KT, Ma E. Acta Mater 2003;51(12):3495–509.
[166] Derlet PM, Hasnaoui A, Van Swygenhoven H. Scripta Mater 2003;49(7):629–35.
[167] Budrovic Z, Van Swygenhoven H, Derlet PM, Van Petegem S, Schmitt B. Science 2004;304(5668):273–6.
[168] Hugo RC, Kung H, Weertman JR, Mitra R, Knapp JA, Follstaedt DM. Acta Mater 2003;51(7):1937–43.
[169] Wu XL, Ma E. Appl Phys Lett 2006;88(23):231911.
[170] Ke M, Hackney SA, Milligan WW, Aifantis EC. Nanostruct Mater 1995;5(6):689–97.
[171] Youngdahl CJ, Weertman JR, Hugo RC, Kung HH. Scripta Mater 2001;44:1475–8.
[172] Shan ZW, Stach EA, Wiezorek JMK, Knapp JA, Follstaedt DM, Mao SX. Science 2004;305(5684):654–7.
[173] Brandstetter S, Budrovic Z, Van Petegem S, Schmitt B, Stergar E, Derlet PM, et al. Appl Phys Lett 2005;87(23):231910.
[174] Youngdahl CJ, Hugo RC, Kung H, Weertman JR. MRS Symp Proc 2001;634:B1.2.1–6.
[175] Chen MW, Ma E, Hemker KJ, Sheng H, Wang Y, Cheng X. Science 2003;300(5623):1275–7.
[176] Liao XZ, Zhao YH, Srinivasan SG, Zhu YT, Valiev RZ, Gunderov DV. Appl Phys Lett 2004;84(4):592–4.
[177] Zhu YT, Liao XZ, Srinivasan SG, Zhao YH, Baskes MI, Zhou F, et al. Appl Phys Lett 2004;85(21):5049–51.
[178] Rosner H, Markmann J, Weissmuller J. Philos Mag Lett 2004;84(5):321–34.
[179] Wang YM, Hodge AM, Biener J, Hamza AV, Barnes DE, Liu K, et al. Appl Phys Lett 2005;86(10):101915.
[180] Wu XL, Zhu YT. Appl Phys Lett 2006;89(3):031922.
[181] Wu X, Zhu YT, Chen MW, Ma E. Scripta Mater 2006;54(9):1685–90.
[182] Yamakov V, Wolf D, Phillpot SR, Mukherjee AK, Gleiter H. Nat Mater 2002;1(1):45–8.
[183] Liao XZ, Zhou F, Lavernia EJ, He DW, Zhu YT. Appl Phys Lett 2003;83(24):5062–4.
[184] Zhu YT, Liao XZ, Srinivasan SG, Lavernia EJ. J Appl Phys 2005;98(3):034319.
[185] Van Swygenhoven H, Derlet PM, Froseth AG. Nat Mater 2004;3(6):399–403.
[186] Jin ZH, Gumbsch P, Ma E, Albe K, Lu K, Hahn H, et al. Scripta Mater 2006;54(6):1163–8.
[187] Pestman BJ, De Hosson JTM, Vitek V, Schapink FW. Philos Mag A 1991;64(4):951–69.
[188] Wang YM, Ma E. Mater Sci Eng A 2004;375(Sp. Iss.):46–52.
[189] Ebrahimi F, Bourne GR, Kelly MS, Matthews TE. NanoStruct Mater 1999;11(3):343–50.
[190] Hirth JP, Lothe J. Theory of dislocations. New York: McGraw-Hill; 1968.
[191] Van Swygenhoven H, Caro A. Phys Rev B 1998;58(17):11246–51.
[192] Ma E. Science 2004;305(5684):623–4.
[193] Evans M, Hastings N, Peacock B. Statistical distributions. New York: John Wiley & Sons; 2000.
[194] Conrad H, Narayan J. Scripta Mater 2000;42(11):1025–30.
[195] Wei YJ, Su C, Anand L. Acta Mater 2006;54(12):3177–90.
[196] Sansoz F, Molinari JF. Scripta Mater 2004;50(10):1283–8.
[197] Sansoz F, Molinari JF. Acta Mater 2005;53(7):1931–44.
[198] Warner DH, Sansoz F, Molinari JF. Int J Plast 2006;22(4):754–74.
[199] Morita T, Mitra R, Weertman JR. Mater Trans JIM 2004;45(2):502–8.
[200] Ebrahimi F, Ahmed Z, Morgan KL. MRS Symp Proc 2001;634:B.2.7.1–6.
[201] Ebrahimi F, Ahmed Z. Mater Charact 2002;49(5):373–9.
[202] Gutkin MY, Ovid'ko IA. Appl Phys Lett 2005;87(25):251916.
[203] Mahajan S, Chin GY. Acta Metall 1973;21(2):173–9.
[204] Christian JW, Mahajan S. Prog Mater Sci 1995;39(1–2):1–157.
[205] Dewald M, Curtin WA. Philos Mag [submitted for publication].
[206] Couzinié JP, Decamps B, Priester L. Philos Mag Lett 2003;83(12):721–31.
[207] Zhu T, Li J, Samanta A, Kim HG, Suresh S. Proc Natl Acad Sci USA 2007;104(9):3031–6.
[208] Henkelman G, Uberuaga BP, Jonsson H. J Chem Phys 2000;113(22):9901–4.
[209] Gutkin MY, Ovid'ko IA. Plastic deformation in nanocrystalline materials. New York: Springer; 2004.